# Invariant manifold growth formula in cylindrical coordinates and its application for magnetically confined fusion

## 柱坐标中不变流形的生长公式及其在磁约束聚变中的应用

**Wenyin Wei** 魏文鉴[1,2,3] wenyin.wei@ipp.ac.cn

**Nov. 24th 2022**

[1]中科院合肥物质研究院，等离子体物理研究所 ***ASIPP***, Institute of Plasma Physics, Chinese Academy of Sciences

[2]中国科学技术大学 ***USTC***, University of Science and Technology of China

[3]德国尤利希研究中心，能源和气候研究所（soon） ***Jülich***, Institut für Energie- und Klimaforschung, Forschungszentrum Jülich GmbH (soon)

# Scope of application

适用范围

- 该篇论文中的公式适用于一次连续可导的向量场，不要求散度为零。
- The formulas in this paper apply to general vector fields of class $C^1$, i.e. once continuously differentiable. The fields does not have to be divergence free.

- 合作推荐格式，标准的 python-numpy 的 npz 文件，文件名任意，
  - Key: 'R', 'Z', 'Phi', 'BR', 'BZ', 'BPhi'
  - Value:
    - 'R', 'Z', 'Phi' keys store the respective 1D axis of the regular equally-spaced grid. Phi: [0, dphi, ...,2pi-dphi,2pi]
    - 'BR', 'BZ', 'BPhi' keys store the respective 3D field component of the grid $[iR, iZ, iPhi]$.

# 目录 Outline

- 背景介绍
  - 嵌套闭合磁面假设
  - 学科分野
  - Poincaré-Hopf 定理
  - Poincaré-Birkhoff 定理
  - 三维磁拓扑相关的实验和模拟研究
  - KAM 定理
  - 现代的共振磁扰动磁谱分析方法
- 流形生长
  - 不变流形的定义
  - 磁力线对初值的敏感性$\mathcal{D}\boldsymbol{X}_{\mathrm{pol}}$
  - $\mathcal{D}\mathcal{P}^{\pm m}$ 在环上的演化和环的分类
  - 生长流形的经典方法和新方法
  - 不变流形的样例演示及解析的例子
- 回顾与展望
  - 边界磁拓扑
  - 最外闭合磁面的确定
  - 拓扑控制

# Nested closed flux surface assumption

## 嵌套闭合磁面假设

**ANSATZ 拟设**

**The torus domain occupied by the bulk plasma is nested by layers of flux surfaces.**
**主体等离子体所处的区域中磁场构成一层层的嵌套磁面。**

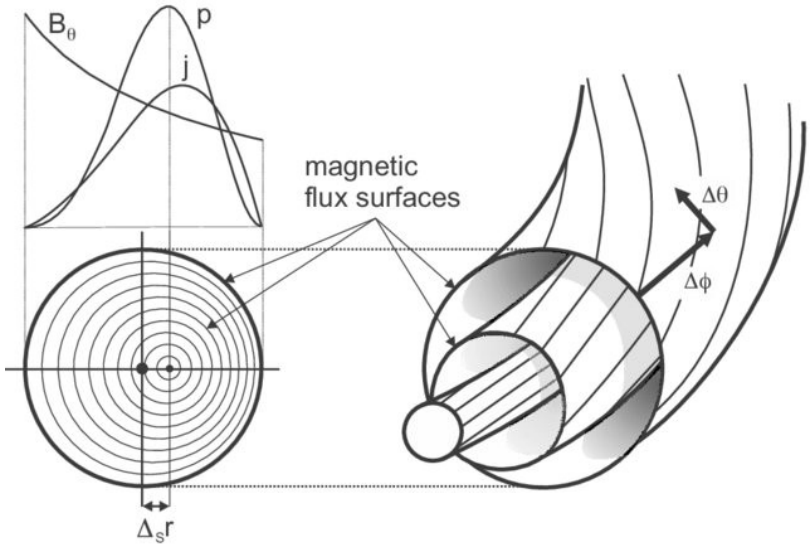


Figure from Jan Willem Coenen, *The Influence of the Dynamic Ergodic Divertor on the Radial Electric Field at the Tokamak TEXTOR* [D] 2009

# Nested closed flux surface assumption broken

## 嵌套闭合磁面假设破缺

图上画的颜色表示磁力线渗透最深处的径向

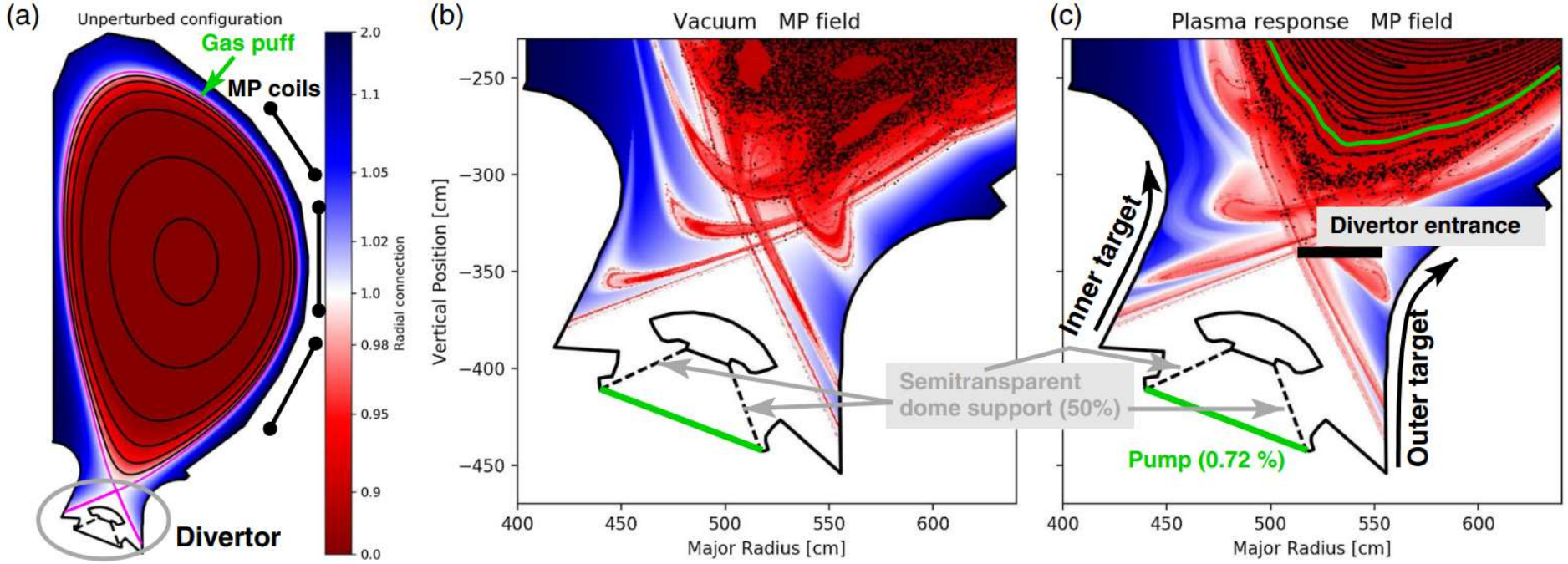


H. Frerichs *et al* 2020 *Phys. Rev. Let.* **125** 155001

Detachment in Fusion Plasmas with Symmetry Breaking Magnetic Perturbation Fields

《加上会打破对称性的扰动场后的聚变等离子体中的脱靶》


Abstract: … However, the divertor plasma regions with connection to the bulk plasma are extended nonaxisymmetrically further outside, where significant heat loads occur, unlike in the symmetric configuration. The temperature remains high at those locations, which reduces the divertor plasma dissipation capacity, making the mitigation of heat loads more difficult to achieve.

然而，连接着主体等离子体的偏滤器等离子体区域被向外非轴对称地延伸出去了，延伸之处会有显著的热负荷，与对称位型是不一样的。这些地方的温度仍然很高，降低了偏滤器等离子体耗散能力，使得减轻热负荷变得更为困难。

# Nested closed flux surface assumption broken

## 嵌套闭合磁面假设破缺

- 这种长期不可预测性是确定性的？还是数值误差积累导致的？
  - 确定性的，是动力系统本身的性质，混沌存在于
    - 三维或以上的连续时间动力系统（即流 flow）
    - 一维或以上的离散时间动力系统（即映射 map）
  - 经典例子是 Lorenz 和 Rossler 吸引子。
- 磁场的散度为零，要如何才能出现混沌？
  - 一开始的混沌研究正是起始于天体物理中的经典多体问题，也是 Hamilton 系统。

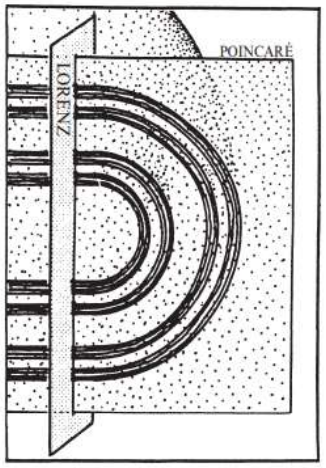


**Figure 12.3.5** Abraham and Shaw (1983), p. 123

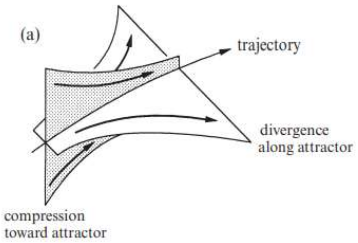


**Figure 12.3.3**

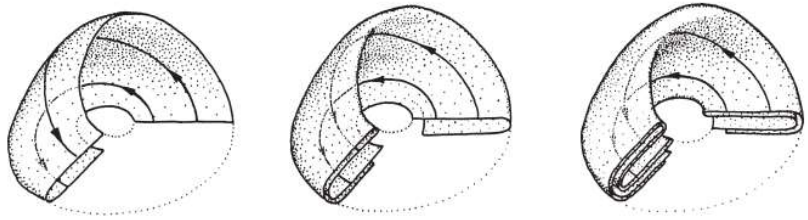


**Figure 12.3.4** Abraham and Shaw (1983), pp 122–123

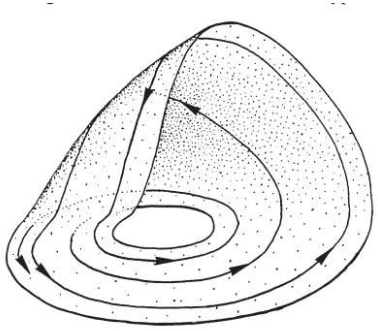

**Figure 12.3.2** Abraham and Shaw (1983), p. 121

# Chaotic or stochastic?

学科分野

## 混沌 chaos

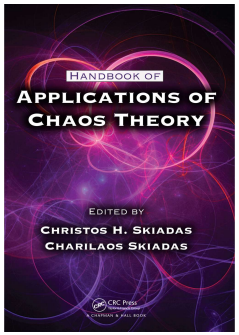


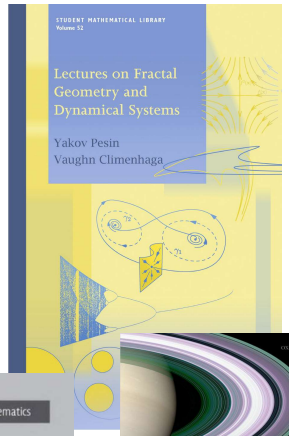


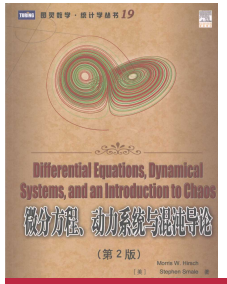


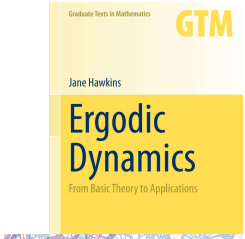


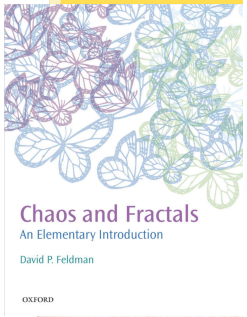


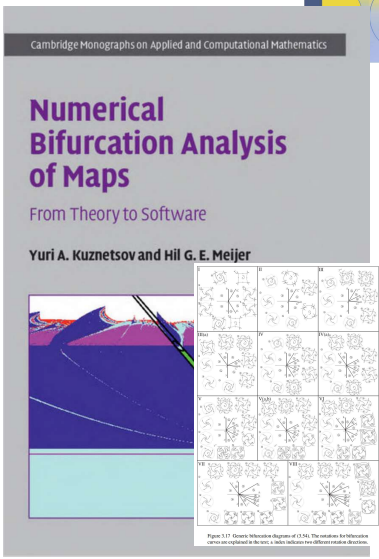


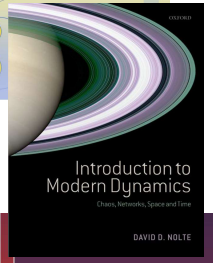


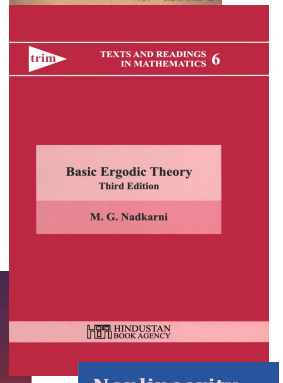


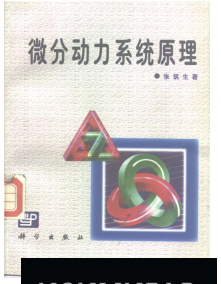


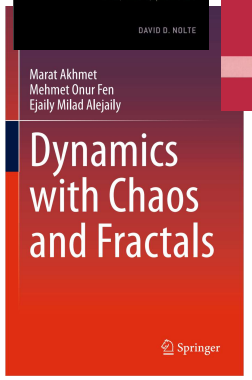


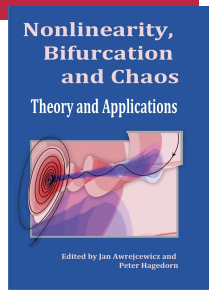


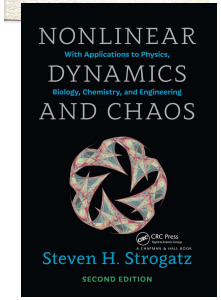


## 随机 stochasticity


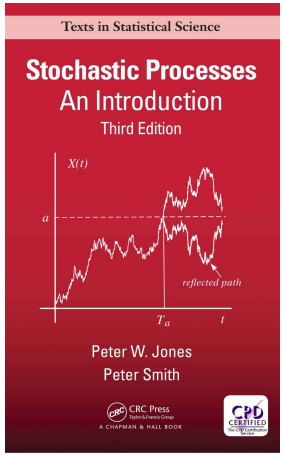


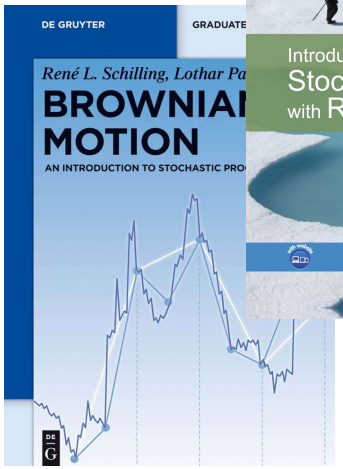


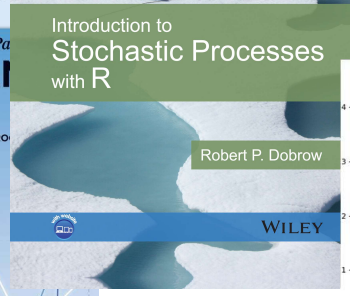


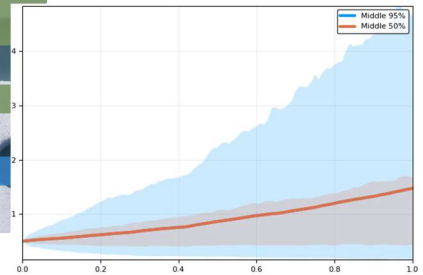


Figure from Julia.DifferentialEquations.jl doc

# Chaotic or stochastic?

学科分野

混沌 chaos

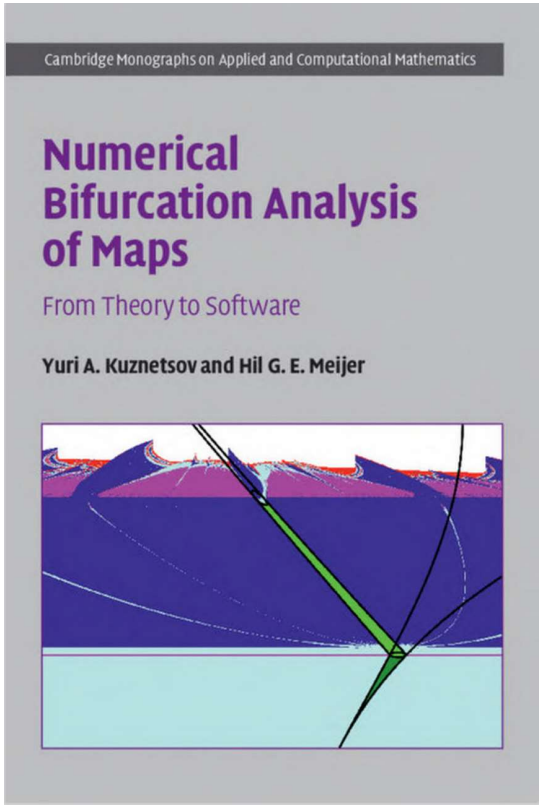


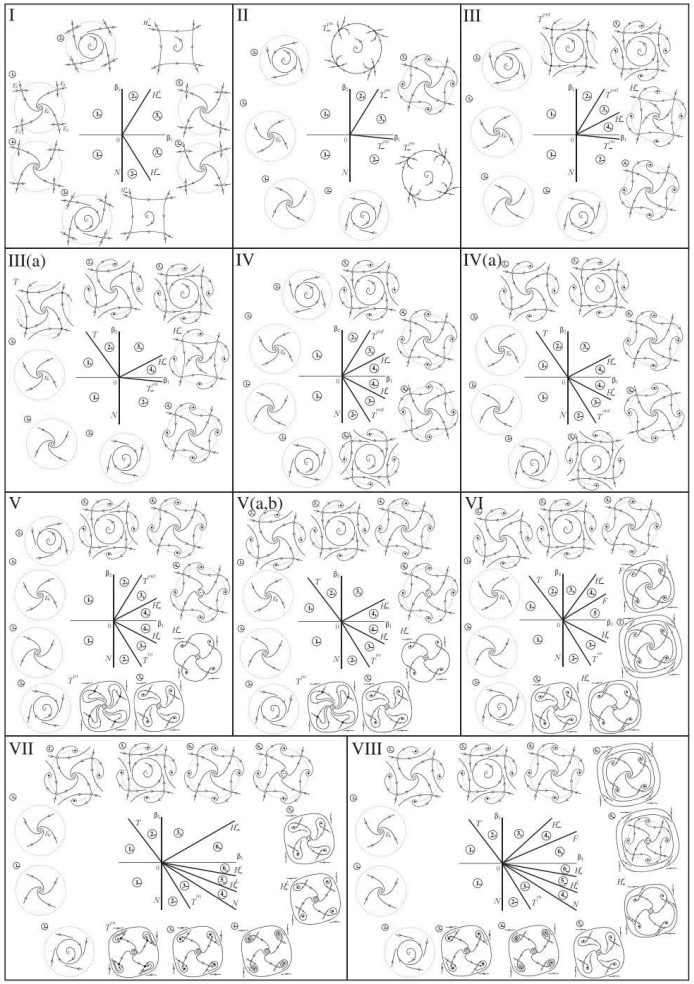


Figure 3.17 Generic bifurcation diagrams of (3.54). The notations for bifurcation curves are explained in the text; ± index indicates two different rotation directions.

# Chaotic or stochastic?

学科分野

## 混沌 chaos

主学科：动力系统和混沌 Dynamical system and chaos

- 主要判据是初值敏感性 Sensitivity to the initial condition
  - 评判初值敏感性的工具
    - Lyapunov 指数（谱）exponent (spectrum)
    - 拓扑熵 topology entropy
- 各态历经性 Ergodic
  - 复现时间 Recurrence time
- 根据 Pugh 的一般稠密性定理（general density theorem），“一般性而言，周期轨在非游离集（non-wandering set）中稠密。”

## 随机 stochasticity

主学科：随机过程 stochastic process

- 主要判据是随机项在方程组中直接引入

Stochastic ordinary/partial differential equations

随机常/偏微分方程

- 公平博弈（鞅） martingale
- 布朗运动 Brown motion
- 伊藤积分 Itô integral



[1]Charles C. Pugh, An Improved Closing Lemma and a General Density Theorem, *Amer. J. Math.* 1967

# Chaotic or stochastic?

## Erratum: Resonant magnetic perturbations of edge-plasmas in toroidal confinement devices (2015 *Plasma Phys. Control. Fusion* 57 123001)

**T E Evans**

General Atomics, PO Box 85608, San Diego, CA 92186–5606, USA

E-mail: evans@fusion.gat.com

of the separatrix. As the strength of the 3D perturbation field increases, the region in the vicinity of the separatrix undergoes transformation to a complex structure in which the field lines mix with each other forming a chaotic or stochastic region surrounding the island lobes. This is a generic prop-

resulting in homoclinic tangles between connected hyperbolic points and heteroclinic tangles between unconnected hyperbolic points [67–70, 72]. These tangles result in stochastic or chaotic field line paths near the hyperbolic points as well as in the boundary of the island defined by the tangle and stochastic tunneling between neighboring islands that can result in global stochasticity [70]. The intersection points between $W^s$

lines. As the amplitude of the perturbation field is increased, these stochastic or chaotic field lines may pass through a significant fraction of stochastic volume or only through a small part depending on the nature of the RMP field and the properties of the axisymmetric equilibrium field. These global 3D stochastic layers have sometimes inappropriately been



Yes, Minister《是，大臣》截图

# Nested closed flux surface assumption broken

## 嵌套闭合磁面假设破缺

- 这种长期不可预测性是确定性的？还是数值误差积累导致的？
  - 确定性的，是动力系统本身的性质，混沌存在于
    - 三维或以上的连续时间动力系统（即流 flow）
    - 一维或以上的离散时间动力系统（即映射 map）
  - 经典例子是 Lorenz 和 Rossler 吸引子。
- 磁场的散度为零，要如何才能出现混沌？
  - 一开始的混沌研究正是起始于天体物理中的经典多体问题，也是 Hamilton 系统。

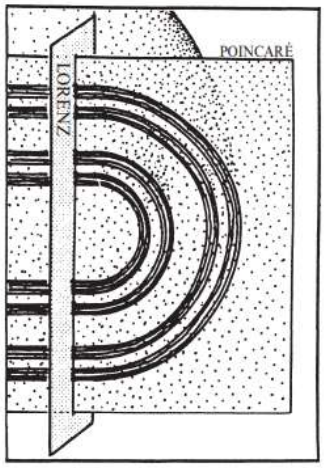


**Figure 12.3.5** Abraham and Shaw (1983), p. 123

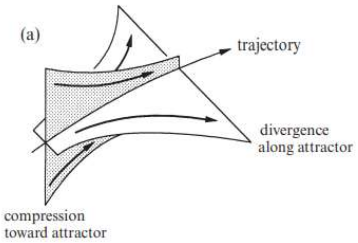


**Figure 12.3.3**

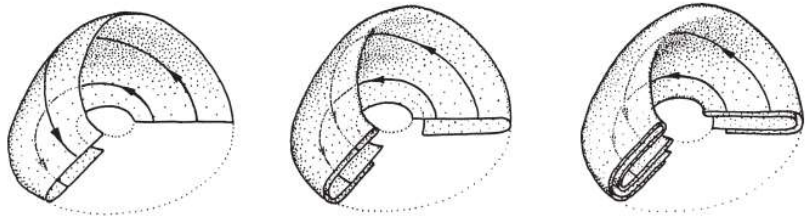


**Figure 12.3.4** Abraham and Shaw (1983), pp 122–123

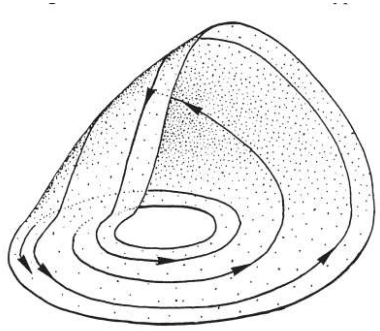

**Figure 12.3.2** Abraham and Shaw (1983), p. 121

# Poincaré-Hopf 定理

## 4.2 环形等离子体位形

### 1. 环形等离子体的性质

如 4.1 节所述，无限长的直圆柱等离子体存在平衡解。虽然这个解可以近似用在一些具体位形，但不是实际的有限区域的严格解。如式 (4-1-1) 这样的平衡方程在有限区域只存在环拓扑解。下面我们说明这个问题。

**环面拓扑** 从式 (4-1-1) 可知，在等离子体边界处，动力压强 $p$ 可以为零，但其梯度不能为零，所以在等离子体表面必须布满磁场，不得有任何漏洞。但是根据法国数学家 H.Poincaré在 19 世纪末提出的一项定理，处处非零的连续向量场必然处在一环拓扑面上。这一定理可在拓扑学中证明，但是我们此处只形象地予以说明。在图 4-2-1(菊池满著，四川大学等离子体物理研究室译，聚变研究物理，科学出版社，2013) 上看到，对于环拓扑面 (a) 和 (b)，无论是环向还是极向的非零向量场 (或两个方向混合) 都可布满曲面，而对于球拓扑面 (c) 和 (d)，这一点却做不到，总有零点出现。对于其他拓扑 (如开两个洞的封闭曲面) 也做不到，因此平衡磁面必然是拓扑环面。

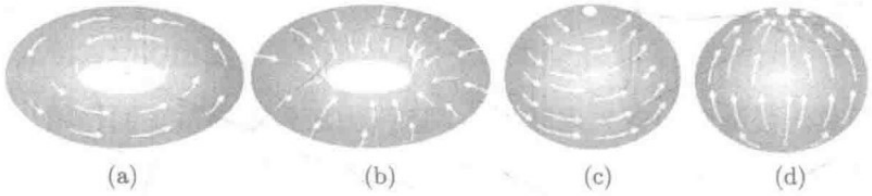


图 4-2-1 不同封闭拓扑曲面上的向量场

这一句换一种说法会更好

“如果一光滑曲面上的光滑切向量场处处非零，则这一曲面必然是亏格为 1 的环面，换言之，微分同胚于标准环面 $\mathbb{T}^2$。”

王龙，《磁约束等离子体实验物理》，科学出版社，2018

# Poincaré-Hopf 定理

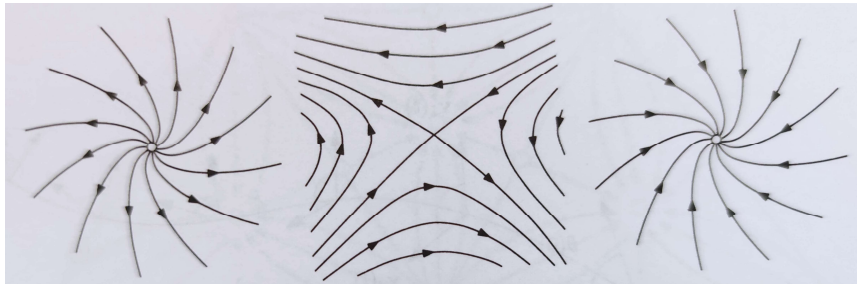

源 source $\iota = +1$　　鞍点 saddle $\iota = -1$　　汇 sink $\iota = +1$

Fig. 向量场零点指标的例子[1]

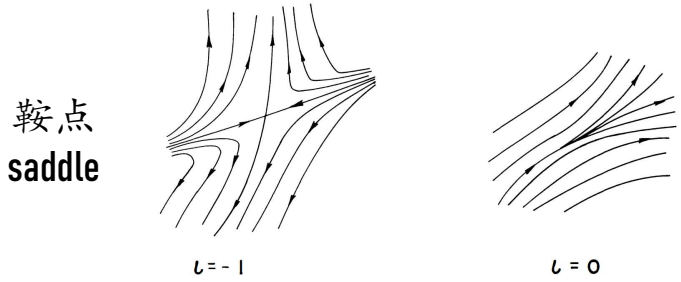


Fig. 向量场零点指标的例子[2]

## THEOREM 定理（Poincaré-Hopf）[1,2]

Let $M$ be a compact orientable smooth manifold and $\boldsymbol{v}$ a smooth (tangent) vector field on $M$ with isolated zeros. If $M$ has a boundary, then $\boldsymbol{v}$ is required to point outward at all boundary points. The sum of the indices of the zeroes of the vector field $\boldsymbol{v}$ on the manifold $M$ equals the manifold's Euler number.

假设 $M$ 是一个紧的可定向光滑流形，$\boldsymbol{v}$ 是该流形上的一个光滑（切）向量场，$\boldsymbol{v}$ 具有孤立零点。如果 $M$ 有边界，向量场就要在边界上指向朝外。则所有孤立零点的指标之和等于该流形的示性数，即

$$\sum_{p \in Z(\boldsymbol{v})} \mathrm{Index}_p(\boldsymbol{v}) = \chi(M)$$

[1] 顾险峰和丘成桐，《计算共形几何（理论篇）》，2020

[2] John W. Milnor, *Topology from the differentiable viewpoint*, The University Press of Virginia, 1965

Poincaré 在 $M$ 二维时证明这一定理，Hopf 1926 年证明完全版本。

# Poincaré-Hopf 定理

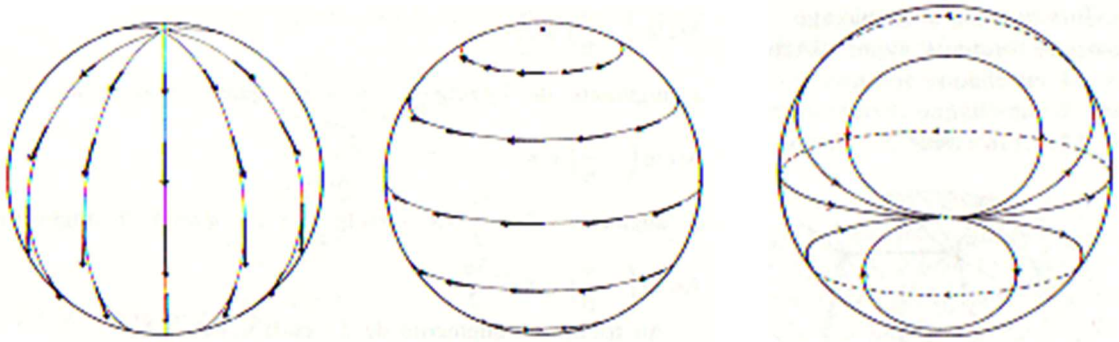

Fig. 标准球的 $\mathbb{S}^2$ 欧拉数为 $\chi = 2$. [2]

Poincaré-Hopf 定理的二维特例又可称为毛球定理 （hairy ball theorem），由布劳威尔在 1912 年证明。

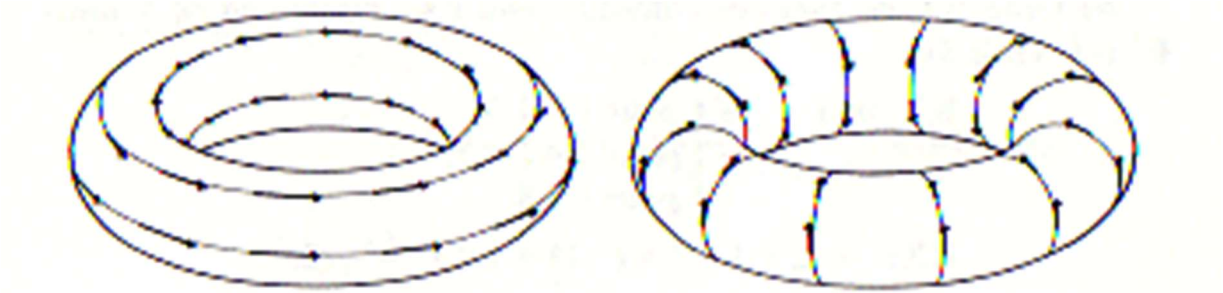

Fig. 标准环的 $\mathbb{T}^2 = \mathbb{S} \times \mathbb{S}$ 欧拉数为 $\chi = 0$. [2]

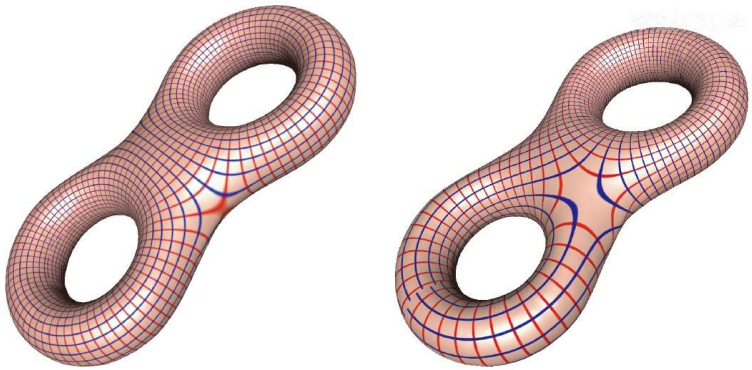

Fig. 亏格为 2 的曲面的欧拉数为 $\chi = -2$. [1]

Euler number for an orientable surface of genus $g$ is $\chi = 2 - 2g$.
一亏格为 $g$ 的可定向曲面的欧拉数为$\chi = 2 - 2g$.

[1] 顾险峰和丘成桐，《计算共形几何（理论篇）》，Fig 6.2，2020

[2] Math Curve, https://mathcurve.com/surfaces.gb/eulerpoincare/eulerpoincare.shtml

# Poincaré-Birkhoff 定理

## THEOREM 定理[1]

**1. Statement of the Theorem.** Poincaré's theorem may be stated in a simple form as follows: Let us suppose that a continuous one-to-one transformation $T$ takes the ring $R$, formed by concentric circles $C_a$ and $C_b$ of radii $a$ and $b$ respectively ($a > b > 0$), into itself in such a way as to advance the points of $C_a$ in a positive sense, and the points of $C_b$ in the negative sense, and at the same time to preserve areas. *Then there are at least two invariant points.*

一个同胚 $T$ 将环带（annulus）$R$ 映到其自身，环带由两个同心圆 $C_a$ 和 $C_b$ 包成，分别半径为 $a$ 和 $b$，$T$ 将这两个同心圆映到其自身，$C_a$ 和 $C_b$ 上的点移动的方向相反，同时 $T$ 还保面积。则有至少两个不动点（fixed point）。

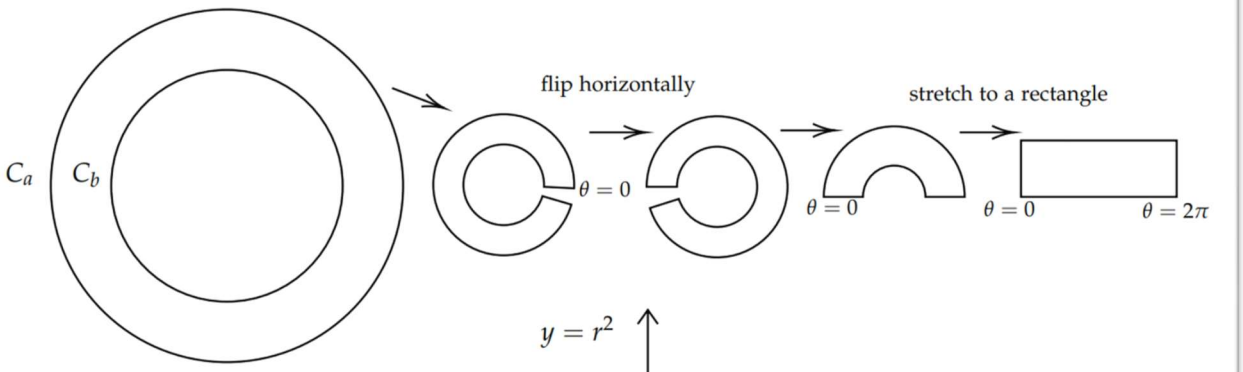


"Points on $C_a$ and $C_b$ are advanced in positive and negative senses, respectively" is said with regard to the lift of $T$ to the semi-plane $\{(\theta, r^2) | r^2 > 0\}$.

## COROLLARY 推论

在嵌套闭合磁面中 $q = m/n$ 的有理面被微扰打破后，邻近的两留存磁面之间必然有 2 个 $\mathcal{P}^m$ 的不动点，一般有 $2km$ 个 $\mathcal{P}$ 的 $m$-周期点。

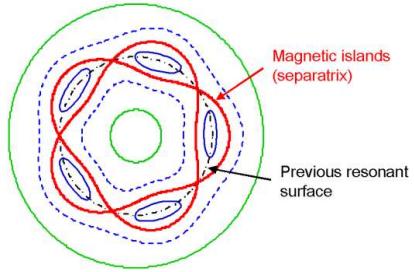


Figure from Eric Nardon doctoral thesis



[1]George D. Birkhoff, Proof of Poincaré's Geometric Theorem, Transactions of the American Mathematical Society ,, **14**, 1, pp. 14-22, 1913

# 3D magnetic topology

## 三维磁拓扑

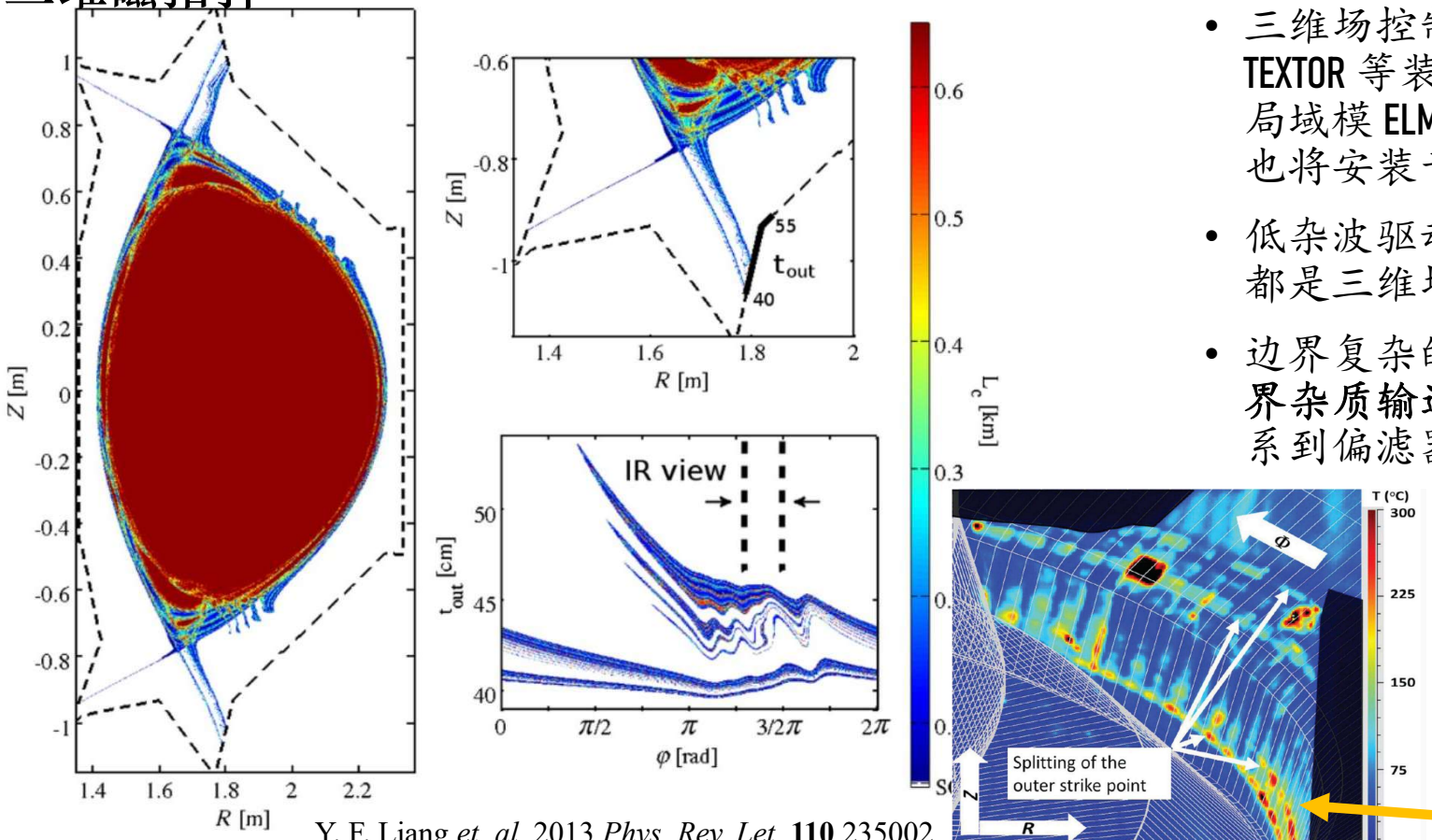


Y. F. Liang *et. al.* 2013 *Phys. Rev. Let.* **110** 235002

- 三维场控制手段已经在 EAST、DIII-D、TEXTOR 等装置上有所研究以探索对边界局域模 ELM 的抑制效果， RMP 线圈预计也将安装于 ITER 上。
- 低杂波驱动的螺旋电流丝、高 m 线圈等都是三维场控制手段。
- 边界复杂的磁拓扑结构对**热流分布**和**边界杂质输运**有重要的研究意义，直接关系到偏滤器的设计。




明显的条带状结构

Fig. EAST 上在低杂波启动时出现打击点分裂现象，对应模拟结果磁力线连接长度分布作图如上 $\phi$=1.3$\pi$, 红外相机对应的视野见右

# 3D magnetic topology

## 三维磁拓扑

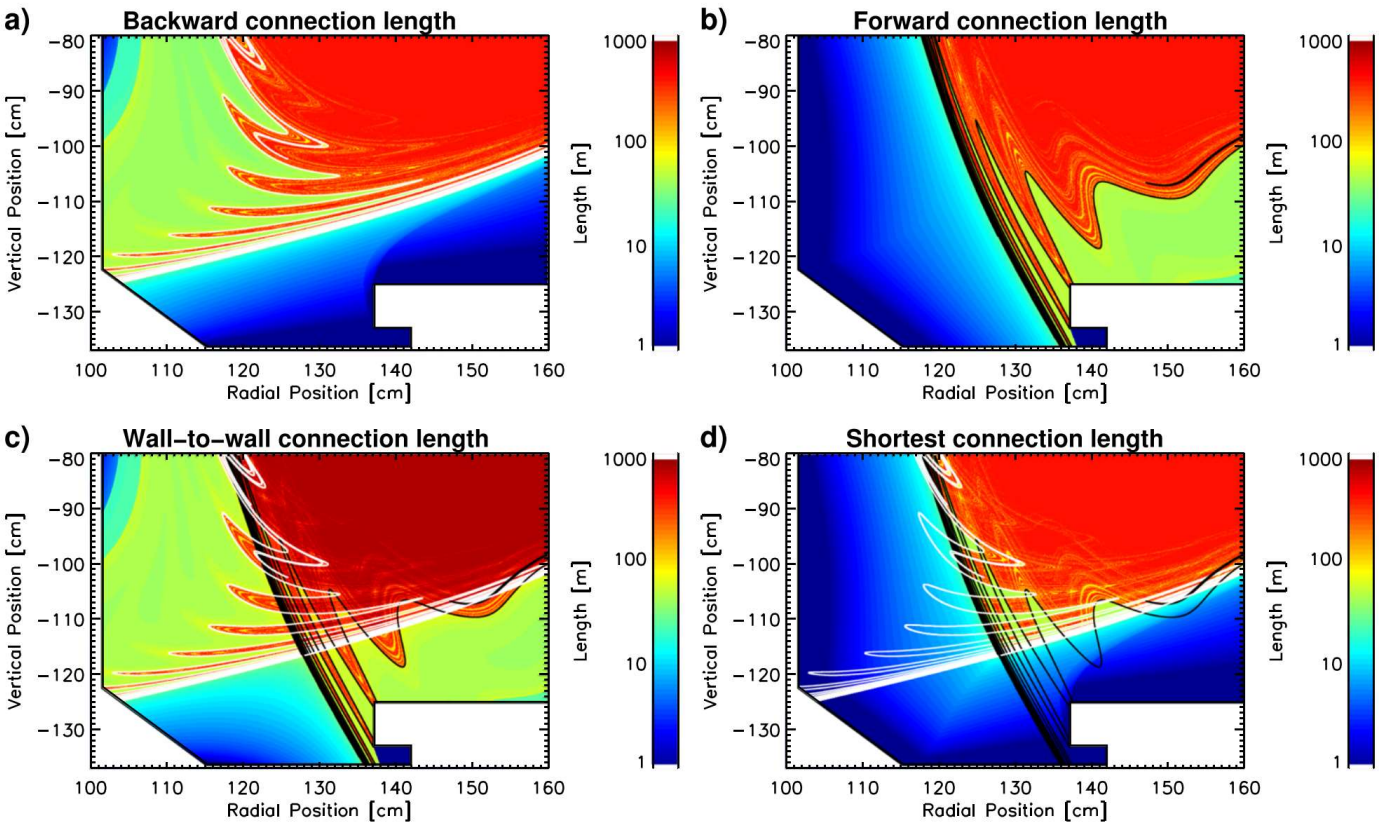


H. Frerichs 2015 *POP* **22** 072508

*The pattern of parallel edge plasma flows due to pressure gradients, recycling, and resonant magnetic perturbations in DIII-D*

*DIII-D* 上由压强梯度、返流、共振磁扰动导致的边界等离子体的平行流的模式

Yuri Kuznetsov, *Numerical bifurcation of maps.* 2020

$$\mathcal{W}^s(S) = \{q \in X |\ f^n(q) \to S \text{ as } n \to \infty\},$$

$$\mathcal{W}^u(S) = \{q \in X |\ f^{-n}(q) \to S \text{ as } n \to \infty\}$$

在动力系统和混沌研究中被称为（稳定/不稳定流形的）**横截相交**，揭示了三维磁拓扑的不平凡。

经典的磁谱分析有其局限性，我们试图在动力系统的基础上，结合聚变的环位形的特殊性，提出系统性的、全域适用的拓扑分析方法。

# 3D magnetic topology

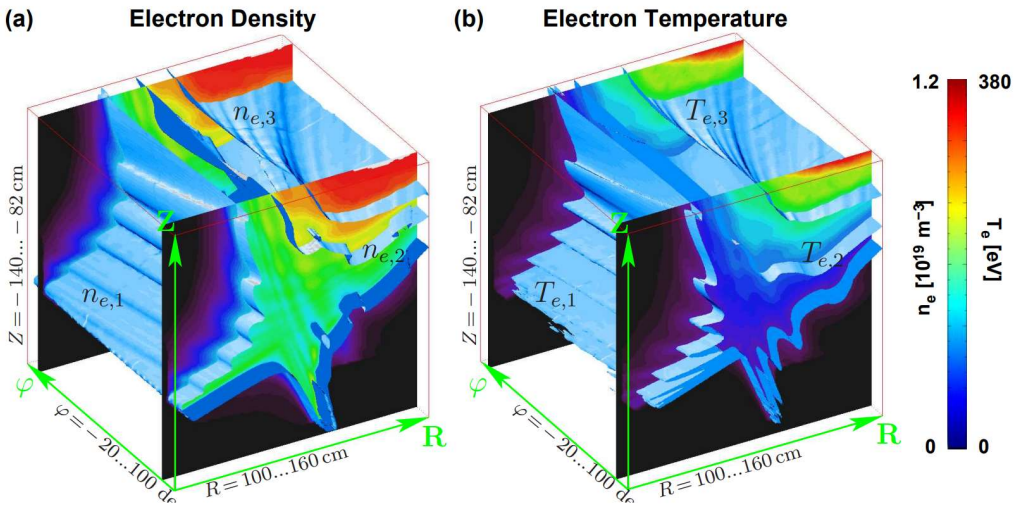


- DIII-D 相关的 EMC3-EIRENE 模拟结果

Heinke Gerd Frerichs, *Three-dimensional plasma transport in open chaotic magnetic fields: A computational assessment for tokamak edge layers* [D] 2010
开放混沌磁场中的三维等离子体输运：对托卡马克边界层的计算评估

- DIII-D 和 EAST 的 EMC3-EIRENE 模拟结果中出现鲜明的横截相交特征

- EMC3 等离子体输运的流体方程
- EIRENE 中性粒子输运的 Monte Carlo 模拟

是国际上常用的三维边界物理模拟工具，能够给出粒子的 $n$、$T$ 分布、靶板上的热流分布、杂质辐射的分布。

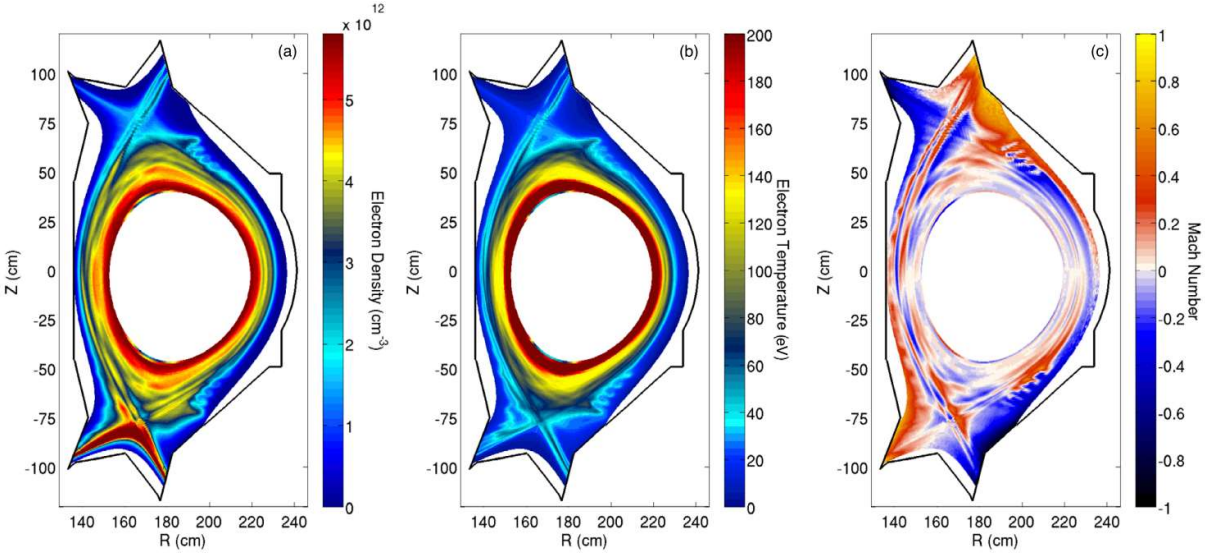


Shuai Xu et al 2018 *Nucl. Fusion* **58** 106008

# KAM 定理

## DEFINITION 定义[1]

Informally speaking, an *integrable system* is a dynamical system with sufficiently many conserved quantities, or first integrals, such that its behaviour has far fewer degrees of freedom than the dimensionality of its phase space; that is, its evolution is restricted to a submanifold within its phase space.

- If there exists a maximal set of conserved quantities, this system is *completely integrable*.

宽松地说，一个**可积系统**是有足够多的守恒量（或首次积分）的动力系统，使得其行为的自由度远低于其所处相空间的维度；换言之，其演化被局限在其相空间的某个子流形中。

- 如果存在最多可能数量的守恒量，该系统被称为**完全可积**。

## COROLLARY 推论[2]

$$\begin{cases} \dot{p} = -\partial_q H(p,q) \\ \dot{q} = \partial_p H(p,q) \end{cases}$$

一般而言，N 个自由度的 2N 维 Hamilton 系统最多拥有 N 个守恒量，这种系统中的轨迹被限制在层叠的 $n$-环上，$n$-环 $\mathcal{T}^n$ 指微分同胚于标准 $n$-环 $\mathbb{T}^n$ 的流形。

KAM theory shows that, under suitable regularity and non-degeneracy assumptions, most (in measure theoretic sense) of invariant $n$-tori persist (slightly deformed) under small Hamiltonian perturbations. The union of persistent $n$-tori (Kolmogorov set) tend to fill the whole phase space as the strength of the perturbation is decreased.

KAM 理论表明，在合适的正则性和非退化性假设前提下，在小的 Hamilton 量扰动下，大部分（从测度论的角度）的不变 $n$-环 $\mathcal{T}^n$ 留存（发生轻微变形）。随着扰动的强度减弱，在扰动下留存的 $n$-环构成的集合（Kolmogorov集）趋向于占据全相空间。

KAM torus 环

[1] Wikipedia contributors. "*Integrable system*." Wikipedia, The Free Encyclopedia. Wikipedia, The Free Encyclopedia, 2022

[2] Luigi Chierchia and John N. Mather (2010) *Kolmogorov-Arnold-Moser theory.* Scholarpedia, 5(9):2123.

# KAM 定理的应用

A final step will bring this into action/angle form. We define

$$u(\psi) = \int_{\psi_a}^{\psi} d\psi'\, q(\psi'), \tag{86}$$

where $\psi_a$ is the value of $\psi$ at the extremal point $a$ of Fig. 1. Then we have the well known form for $\mathbf{B}_0$,

逆变基×逆变基→协变基

$$\mathbf{B}_0 = \nabla u \times \nabla\theta - \nabla\psi \times \nabla\phi. \tag{87}$$

A vector potential for this is

逆变基

$$\mathbf{A}_0 = u\nabla\theta - \psi\nabla\phi, \tag{88}$$

which can be written as a 1-form,

微分 1-形式

$$\gamma_0 = \mathbf{A}_0 \cdot d\mathbf{x} = u\, d\theta - \psi\, d\phi. \tag{89}$$

正则角度/作用量

This is in the canonical action/angle form, $Jd\theta - H(J)\,dt$. Thus, $u$ and $\theta$ are action/angle variables for the unperturbed field line flow, and $\psi = \psi(u)$ is the Hamiltonian.

磁通作为哈密顿量

The equations of motion in the variables $(u, \theta, \phi)$ are given by Hamilton's equations

磁力线的 Hamilton 形式

$$\frac{d\theta}{d\phi} = \frac{\partial\psi}{\partial u} = \frac{1}{q}, \qquad \frac{du}{d\phi} = -\frac{\partial\psi}{\partial\theta} = 0. \tag{90}$$

The field line flow consists of straight lines in the coordinates $(u, \theta, \phi)$.

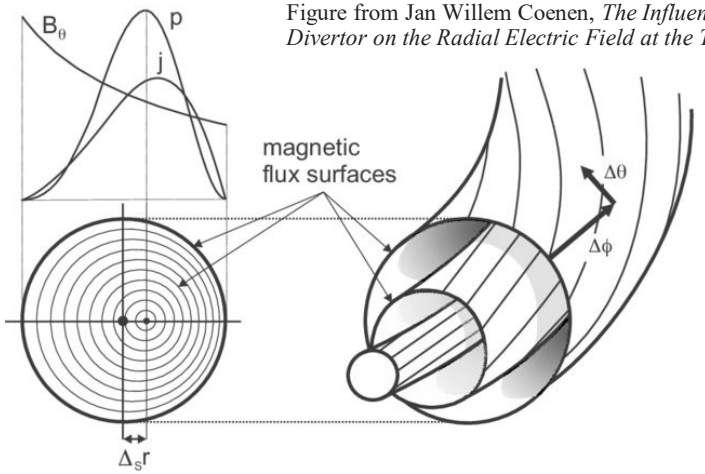


Figure from Jan Willem Coenen, *The Influence of the Dynamic Ergodic Divertor on the Radial Electric Field at the Tokamak TEXTOR* [D] 2009

一般而言，N 个自由度的 2N 维 Hamilton 系统最多拥有 N 个守恒量，这种系统中的轨迹被限制在层叠的 $n$-环上，$n$-环 $\mathcal{T}^n$ 指微分同胚于标准 $n$-环 $\mathbb{T}^n$ 的流形。

John R. Cary and Robert G. Littlejohn, *Annals of Physics* **151**, 1-34, 1983
Noncanonical Hamiltonian Mechanics and Its Application to Magnetic Field Line Flow
非正则哈密顿力学和其对于磁力线流动的应用

# Modern RMP

All figures in this slide, except the top right one, are from Eric Nardon doctoral thesis, https://www.osti.gov/etdeweb/servlets/purl/21120950

ASIPP

## 现代的共振磁扰动

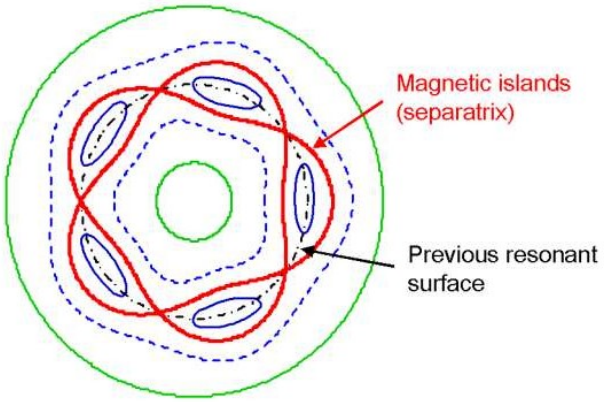


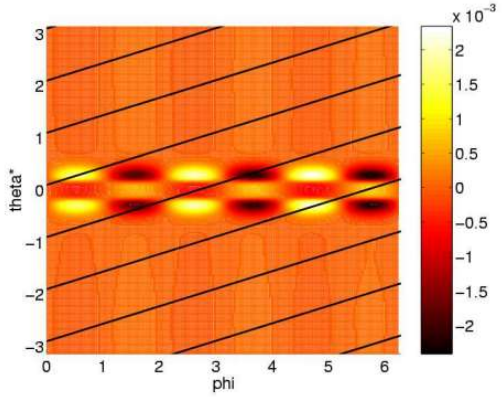


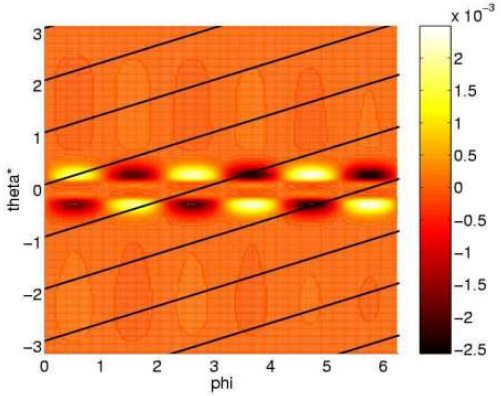


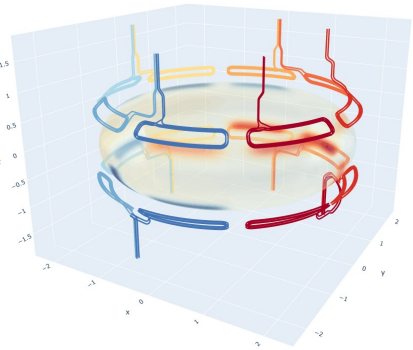

Fig. $B^r$ on EAST

Figure 3.11: Colormap of $B^1/B^3$ (dimensionless quantity) on the $q = 3$ equilibrium flux surface, together with several field lines. Left: I-coils even parity (1kAt). Right: I-coils odd parity (1kAt).

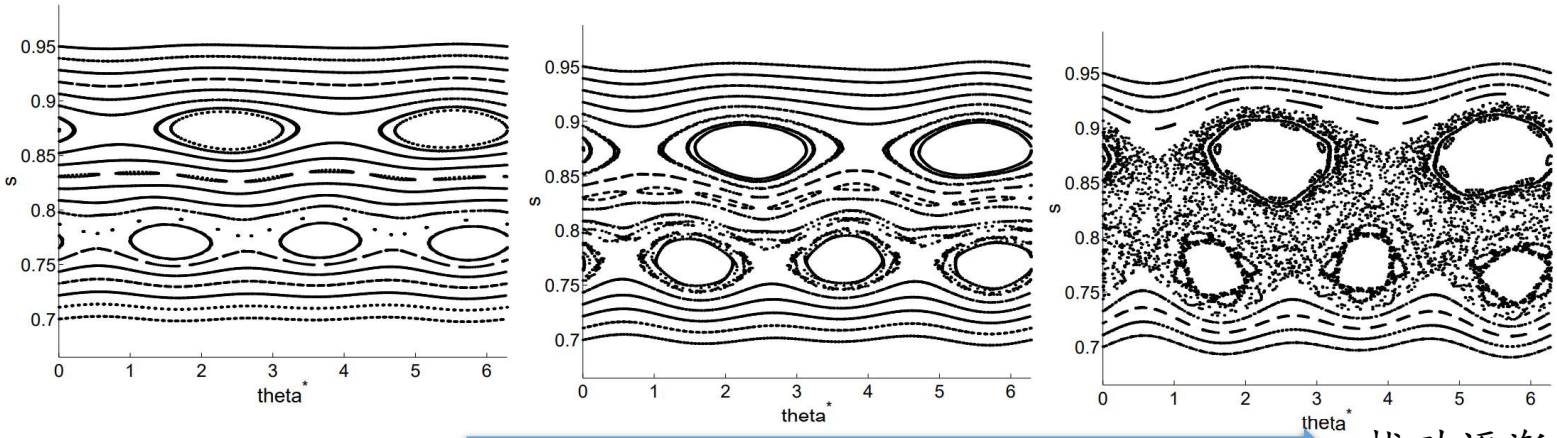


扰动逐渐变大

Chirikov parameter 参数

$$\sigma_{Chir}^{m,m+1} \equiv \frac{\delta_{q=m/n} + \delta_{q=(m+1)/n}}{\Delta_{m,m+1}}$$

# Modern RMP

Eric Nardon doctoral thesis,
https://www.osti.gov/etdeweb/servlets/purl/21120950

ASIPP



现代的共振磁扰动

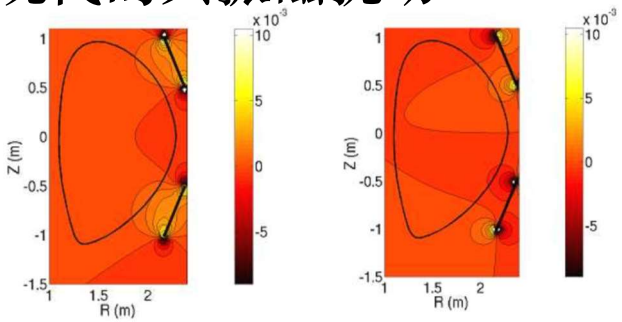


Figure 3.1: Poloidal cuts (in the plane $\varphi = 30°$, which approximately corresponds to the middle of a coil) of $B^R$ (left) and $B^Z$ (right) produced by the I-coils fed with 1kAt, in Teslas. The I-coils appear as black bars, and the plasma separatrix is also represented.

this discharge are a major radius $R_0 = 1.72$m, a triangularity (see [2] for a definition) $\langle\delta\rangle \simeq 0.5$, an elongation [2] $\kappa = 1.78$, a toroidal field on axis $B_0 = 1.9$T, a plasma current $I_p = 1.55$MA, and a safety factor at $s = 0.95^{1/2}$ (see just below for the definition of $s$) $q_{95} = 3.5$. The magnetic equilibrium and all metric coefficients are calculated using the HELENA code [42]. We work in the intrinsic equilibrium coordinates $(s, \theta^*, \varphi)$, where $s \equiv \psi^{1/2}$ ($\psi$ being the normalized poloidal magnetic flux, cf. introduction) is used as a radial coordinate (in the $(s, \theta^*, \varphi)$ system of coordinates, a flux surface is defined by $s = cte$, in particular $s = 0$ for the magnetic axis and $s = 1$ for the separatrix[1]), and $\theta^*$ is such that field lines are straight in the $(s, \theta^*, \varphi)$ system of coordinates:

$$\left.\frac{d\varphi}{d\theta^*}\right|_{FL} = q, \tag{3.2}$$

where the derivative is taken along a field line. We define:

$$B^1 \equiv \vec{B}\cdot\vec{\nabla}s, \tag{3.3}$$
$$B^2 \equiv \vec{B}\cdot\vec{\nabla}\theta^*, \tag{3.4}$$
$$B^3 \equiv \vec{B}\cdot\vec{\nabla}\varphi, \tag{3.5}$$

and our radial-like normalized magnetic perturbations have the following expression:

$$b^r \equiv \frac{b^1}{\sqrt{g^{11}}}, \tag{3.6}$$

[1]It is usual to work with $\psi^{1/2}$ instead of $\psi$ as a radial coordinate (although $\psi$ is sometimes used) because for a cylindrical plasma with a spatially constant axial current density, $\psi^{1/2}$ exactly corresponds to the normalized radius $r/a$, where $a$ is the plasma minor radius.



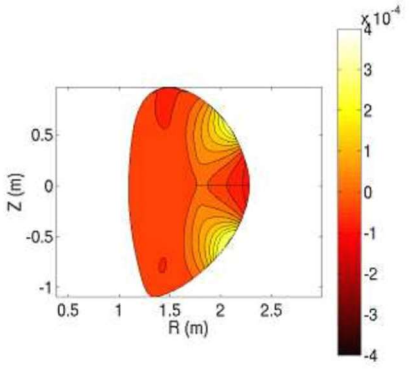


Figure 3.2: Poloidal cut (in the plane $\varphi = 30°$, as in 3.1) of $b^r$ (dimensionless quantity) produced by the I-coils in even parity configuration fed with 1kAt.

where $b^1 \equiv B^1/B_0$ ($B_0$ being the vacuum toroidal magnetic field on the geometrical axis) and $g^{11} \equiv \vec{\nabla}s\cdot\vec{\nabla}s$. A poloidal cut of $b^r$ produced by the I-coils in even parity configuration is shown in fig. 3.2.

### 3.2.3 Calculation of the resonant harmonics

Next step consists in calculating the Fourier spectrum of the radial-like magnetic perturbations with respect to the toroidal angle $\varphi$ and intrinsic poloidal angle $\theta^*$. More exactly, one needs to calculate the Fourier spectrum of

$$\tilde{b}^1 \equiv B^1/B^3, \tag{3.7}$$

with $B^3 \equiv \vec{B}\cdot\vec{\nabla}\varphi$, because it is the resonant harmonics of $\tilde{b}^1$ that appear in the expression of the islands widths. This is demonstrated in appendix A). We define:

$$\tilde{b}^1_{mn}(s) \equiv \int_{\varphi=0}^{2\pi}\int_{\theta^*=0}^{2\pi} \tilde{b}^1(s,\theta^*,\varphi)\, e^{-i(m\theta^*+n\varphi)}\frac{d\theta^*}{2\pi}\frac{d\varphi}{2\pi}, \tag{3.8}$$

so that:

$$\tilde{b}^1(s,\theta^*,\varphi) = \sum_{m,n=-\infty}^{\infty} \tilde{b}^1_{mn}(s) e^{i(m\theta^*+n\varphi)}. \tag{3.9}$$

It should be noticed that, because $\tilde{b}^1$ is a real number, we have:

$$\tilde{b}^1_{-m,-n} = \left(\tilde{b}^1_{mn}\right)^*, \tag{3.10}$$

Fig. Two pages from Eric Nardon's doctoral thesis.

## Eric denotation -> MHDpy variable name

- $(s, \theta^*, \phi)$ -> (S, TET, Phi)
- Subscript -> single underscore
- Superscript -> double underscore
- $B^1$ -> B__1
- $\tilde{b}^1$ -> tilde_b__1
- $\tilde{b}^1_{mn}$ -> tilde_b_mn__1

# Modern RMP

## 现代共振磁扰动

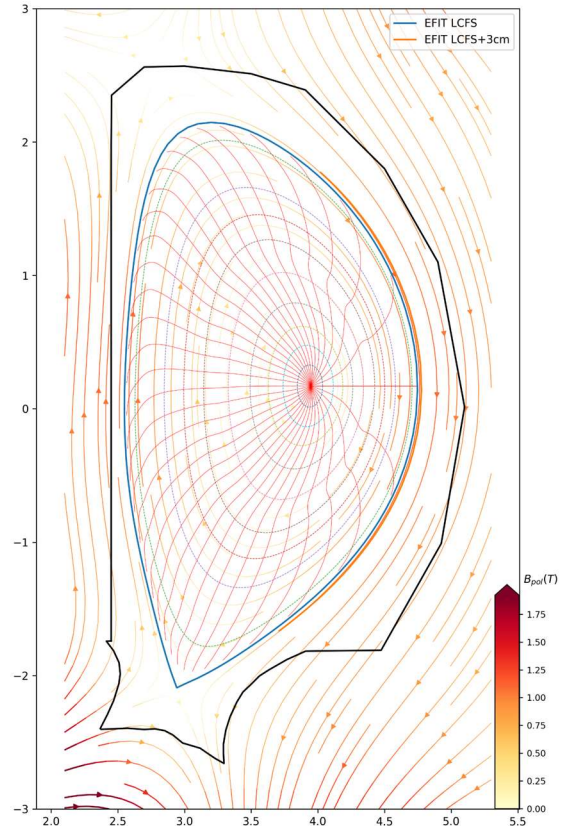


Fig. BEST $(s, \theta^*, \phi)$ mesh.

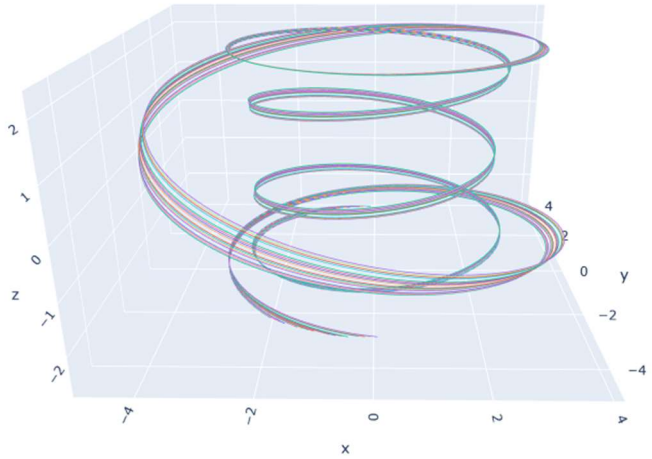

Fig. How the 16 HCFs induced by port K LHW look like.

低杂波激励产生的螺旋电流丝形状

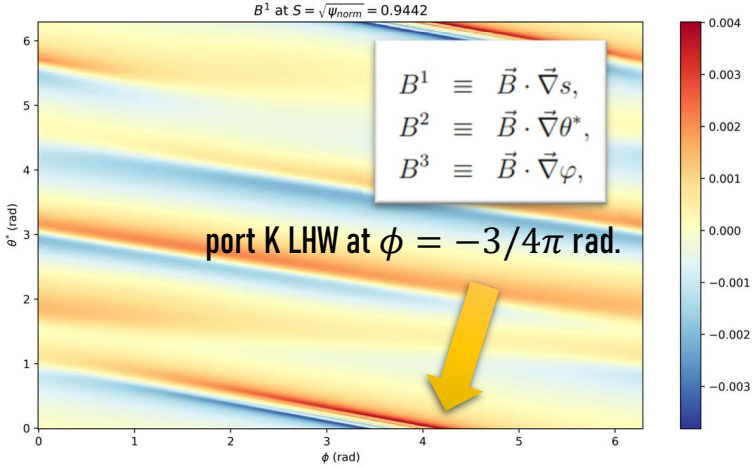


Fig. $B^1$ of the HCFs induced by port K LHW at a flux surface.

在 K 端低杂波激励下产生的 4 根螺旋电流丝对应的 $B^1$ 分量

$\mathbf{2|\tilde{b}^1_{mn}| * 10^4}$ 从里到外

$$\tilde{b}^1 \equiv B^1/B^3,$$

$$\tilde{b}^1_{mn}(s) \equiv \int_{\varphi=0}^{2\pi} \int_{\theta^*=0}^{2\pi} \tilde{b}^1(s, \theta^*, \varphi)\, e^{-i(m\theta^* + n\varphi)} \frac{d\theta^*}{2\pi} \frac{d\varphi}{2\pi},$$

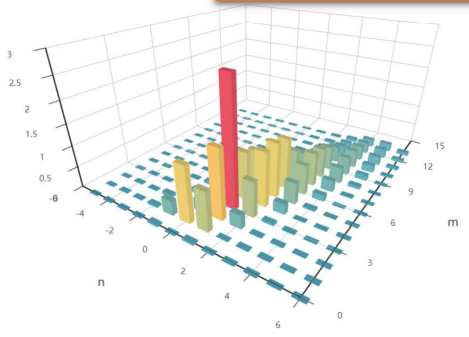

$@S = 0.7285$

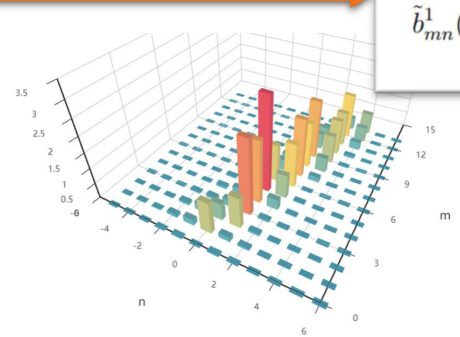

$@S = 0.9442$

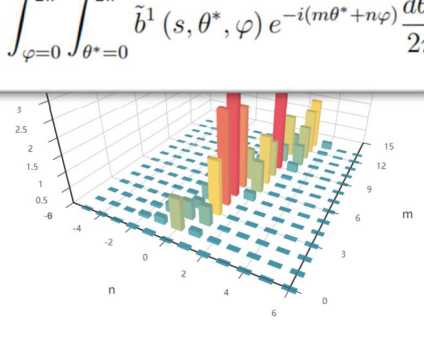

$@S = 0.9821$

# Modern RMP

## 现代共振磁扰动

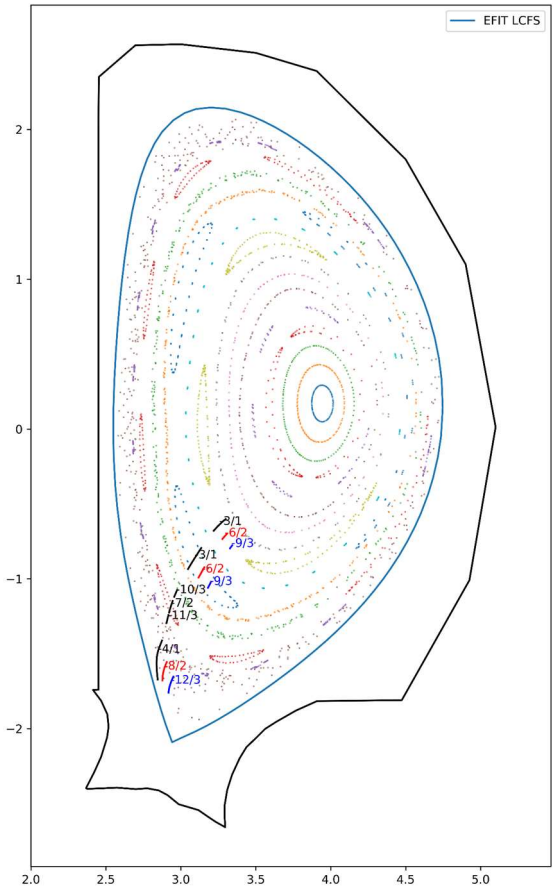


Fig. BEST + 5kA HCF Poincaré plot

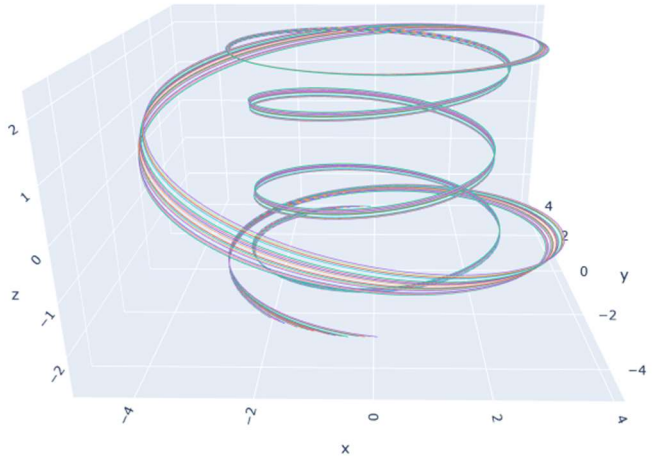

Fig. How the 16 HCFs induced by port K LHW look like.

低杂波激励产生的螺旋电流丝形状

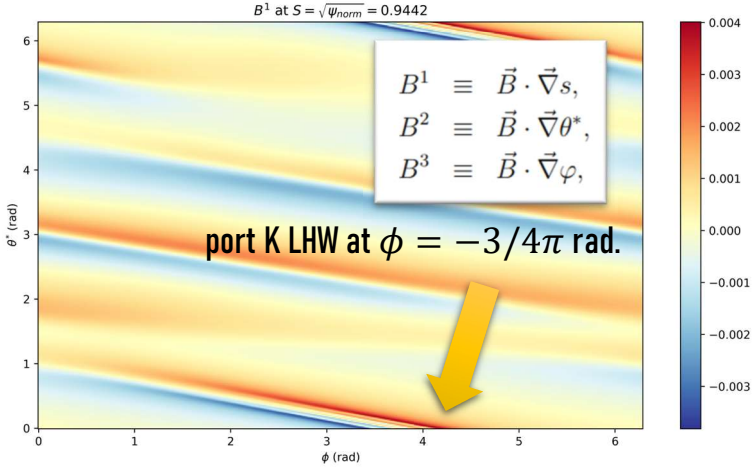


Fig. $B^1$ of the HCFs induced by port K LHW at a flux surface.

在 K 端低杂波激励下产生的 4 根螺旋电流丝对应的 $B^1$ 分量

$$2|\tilde{b}^1_{mn}| * 10^4$$ 从里到外

$$\tilde{b}^1 \equiv B^1/B^3,$$

$$\tilde{b}^1_{mn}(s) \equiv \int_{\varphi=0}^{2\pi}\int_{\theta^*=0}^{2\pi} \tilde{b}^1(s,\theta^*,\varphi)\, e^{-i(m\theta^*+n\varphi)}\frac{d\theta^*}{2\pi}\frac{d\varphi}{2\pi},$$

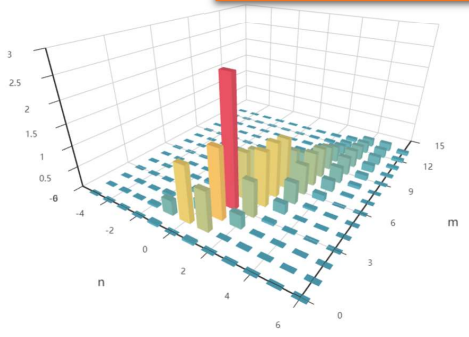

$@S = 0.7285$

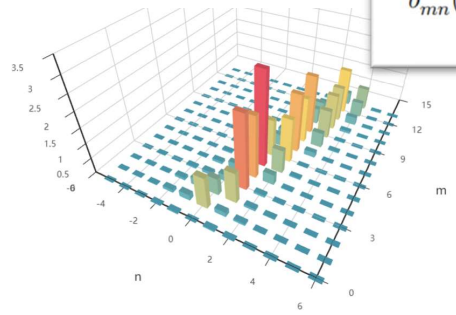

$@S = 0.9442$

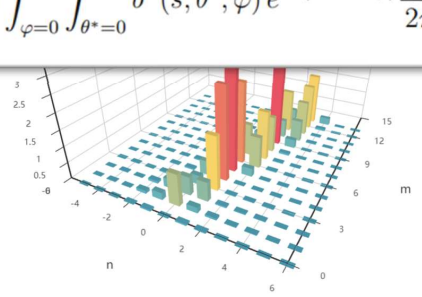

$@S = 0.9821$

# Modern RMP

## 现代共振磁扰动

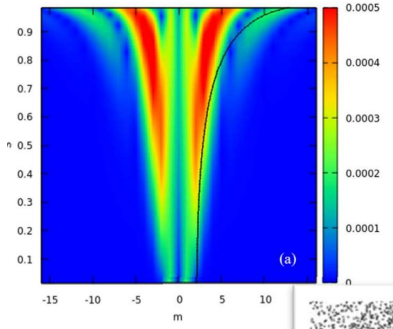


Fig. 典型的磁谱分析，EAST 上的扰动场径向分量的 Fourier 磁谱 n=2，RMP 偶宇称（$I_{RMP} = 5kA$）

Jie Huang *et al* 2019 *Plasma Sci. Technol.* **21** 065105

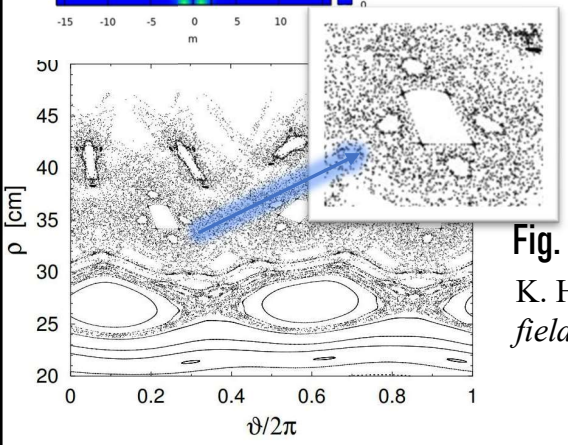


Fig. TEXTOR 上 #94809 炮的 Poincare 图

K. H. Finken *et al* 2005 *The structure of magnetic field in TEXTOR-DED*

Fig. 对极向偏滤器位型，TRIP_MAP 给出 X 点周围的的流形叠加在 Poincare 图上

T. E. Evans *et al* 2005 *J. Phys.: Conf. Ser.* **7** 015

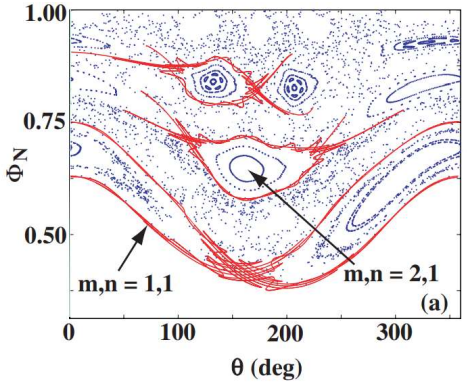


- 顾里不顾外
  - 分界面外
  - 混沌场区
- 多模式耦合(异宿相交)面对的困难
  - 磁力线追踪在 Poincaré 图上离散分布，难以看出层次性的结构特征。
  - 难以定位残余的磁位垒。
  - 磁岛链 X 点周围的**混沌化**程度难以刻画。
  - Fourier 变换是线性操作，只能揭示小扰动

$$\mathcal{F}(a\boldsymbol{f} + b\boldsymbol{g}) = a\mathcal{F}(\boldsymbol{f}) + b\mathcal{F}(\boldsymbol{g})$$

Evans 等人已经基于朴素的迭代方法获得了随机场区中 X 点生出流形的结构，我们更近一步，结合聚变的环位形的特殊性，提出其流形的生长方程，系统性地构建三维磁拓扑的结构和控制理论。

# 目录 Outline

- 背景介绍
  - 嵌套闭合磁面假设
  - 学科分野
  - Poincaré-Hopf 定理
  - Poincaré-Birkhoff 定理
  - 三维磁拓扑相关的实验和模拟研究
  - KAM 定理
  - 现代的共振磁扰动磁谱分析方法
- 流形生长
  - 不变流形的定义
  - 磁力线对初值的敏感性$\mathcal{D}\boldsymbol{X}_{\mathrm{pol}}$
  - $\mathcal{D}\mathcal{P}^{\pm m}$ 在环上的演化和环的分类
  - 生长流形的经典方法和新方法
  - 不变流形的样例演示及解析的例子
- 回顾与展望
  - 边界磁拓扑
  - 最外闭合磁面的确定
  - 拓扑控制

# Invariant manifold definitions

## 不变流形的定义

**DEFINITION 定义**

An *invariant* set $S$ under $\boldsymbol{f}$ means that once an orbit of $\boldsymbol{f}$ enters the set S, it can never go out of $S$.
如果 $\boldsymbol{f}$ 作用下的任何轨迹进入一集合 $S$ 后，这些轨迹都不会再离开这一集合，则称 $S$是 $\boldsymbol{f}$ 下的**不变集**。

**DEFINITION 定义**

Let $S$ be a hyperbolic invariant set under $\boldsymbol{f}$, then the stable and unstable manifolds are defined by:
令 $S$ 为 $\boldsymbol{f}$ 作用下一双曲不变集，则 $S$ 的稳定、不稳定流形分别定义为：

$$\mathcal{W}^s(S) := \{\boldsymbol{p} \in M \mid \omega(\boldsymbol{p}) = S\},$$
$$\mathcal{W}^u(S) := \{\boldsymbol{p} \in M \mid \alpha(\boldsymbol{p}) = S\},$$

Yuri Kuznetsov, *Numerical bifurcation of maps.* 2020

$$\mathcal{W}^s(S) = \{q \in X \mid f^n(q) \to S \text{ as } n \to \infty\},$$
$$\mathcal{W}^u(S) = \{q \in X \mid f^{-n}(q) \to S \text{ as } n \to \infty\}$$

什么是极限集？

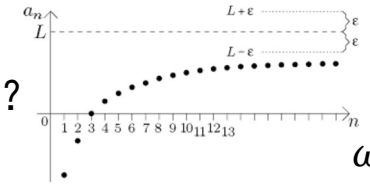

错叠

$\omega = \{L_1\}$

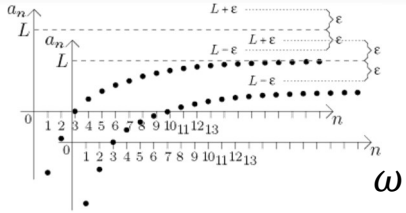

再错叠

$\omega = \{L_1, L_2\}$

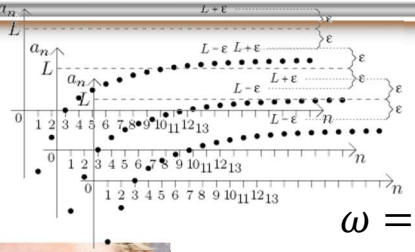

$\omega = \{L_1, L_2, L_3\}$

为什么要叫 $\alpha$ 极限集、$\omega$ 极限集？
为什么用符号 $\mathcal{W}$？

$\alpha\ \beta\ \gamma\ \delta\ \varepsilon\ \ldots\ \varphi\ \phi\ \chi\ \psi\ \omega$
Wrinkle 皱纹、褶皱

Fig. 用 wrinkle 搜索到的网图[1]

[1]Organic Beauty Report

# Field line tracing sensitivity to the initial condition

## 磁力线追踪对起始点的敏感性

$$\dot{\boldsymbol{x}} = \boldsymbol{B}(\boldsymbol{x}) \Rightarrow \begin{cases} \mathrm{d}x_R/\mathrm{d}t = B_R \\ \mathrm{d}x_Z/\mathrm{d}t = B_Z \\ \mathrm{d}x_\phi/\mathrm{d}t = B_\phi/R \end{cases}$$

$$\begin{cases} x = R\cos\phi \\ y = R\sin\phi \\ z = Z \end{cases}$$

$$\begin{cases} \mathrm{d}x_R/\mathrm{d}x_\phi = RB_R/B_\phi \\ \mathrm{d}x_Z/\mathrm{d}x_\phi = RB_Z/B_\phi \end{cases}$$

- 这个非自治连续时间动力系统的解记作

$$\boldsymbol{X}_{pol}(\boldsymbol{x}_0, \phi_s, \phi_e)$$

$$\frac{\partial}{\partial \phi_e}\boldsymbol{X}_{pol}(\boldsymbol{x}_0, \phi_s, \phi_e) = \frac{R\boldsymbol{B}_{pol}}{B_\phi}\left(\boldsymbol{X}_{pol}(\boldsymbol{x}_0, \phi_s, \phi_e), \phi_e\right)$$

- 对初值的导数记作 $\mathcal{D}\boldsymbol{X}_{pol}(\boldsymbol{x}_0, t) := \partial \boldsymbol{X}_{pol}(\boldsymbol{x}_0, t)/\partial(x_{0R}, x_{0Z})$

套一下链式法则，就得到了

$$\frac{\partial}{\partial \phi_e}\mathcal{D}\boldsymbol{X}_{pol}(\boldsymbol{x}_0, \phi_s, \phi_e) = \frac{\partial R\boldsymbol{B}_{pol}/B_\phi}{\partial(R,Z)}(\boldsymbol{X}_{pol}(\boldsymbol{x}_0, \phi_s, \phi_e), \phi_e)\,\mathcal{D}\boldsymbol{X}_{pol}(\boldsymbol{x}_0, \phi_s, \phi_e)$$

这个矩阵经常会用，简记作 $\mathbf{A}(\phi) := \frac{\partial\left(R\boldsymbol{B}_{pol}/B_\phi\right)}{\partial(R,Z)}(\boldsymbol{X}_{pol}(\boldsymbol{x}_0, \phi_s, \phi), \phi)$

$$\frac{\partial}{\partial \phi_e}\mathcal{D}\boldsymbol{X}_{pol}(\phi_s, \phi_e) = \mathbf{A}(\phi_e)\,\mathcal{D}\boldsymbol{X}_{pol}(\phi_s, \phi_e)$$

# Field line tracing sensitivity to the initial condition

## 磁力线追踪对起始点的敏感性

$$\dot{x} = B(x)$$

如果 $B_\phi$ 在这条磁力线上会变号，经过零，也就是环向反转，如何处理？退回到笛卡尔坐标系。

$$\left[\begin{matrix}1 & & -\frac{RB_R}{B_\phi}\\ & & \\ & 1 & -\frac{RB_Z}{B_\phi}\end{matrix}\right]\Bigg|_{end}\left[\begin{matrix}\cos\phi & & -R\sin\phi\\ \sin\phi & & R\cos\phi\\ & 1 & \end{matrix}\right]\Bigg|_{end}^{-1}\mathcal{D}X\left[\begin{matrix}\cos\phi & & -R\sin\phi\\ \sin\phi & & R\cos\phi\\ & 1 & \end{matrix}\right]\Bigg|_{start}=\left[\begin{matrix}\mathcal{D}X_{pol} & \begin{matrix}*\\ *\end{matrix}\end{matrix}\right]$$

$$\frac{\partial}{\partial\phi_e}X_{pol}(x_0,\phi_s,\phi_e)=\frac{RB_{pol}}{B_\phi}\left(X_{pol}(x_0,\phi_s,\phi_e),\phi_e\right)$$

- 对初值的导数记作 $\mathcal{D}X_{pol}(x_0,t):=\partial X_{pol}(x_0,t)/\partial(x_{0R},x_{0Z})$

套一下链式法则，就得到了

$$\frac{\partial}{\partial\phi_e}\mathcal{D}X_{pol}(x_0,\phi_s,\phi_e)=\frac{\partial RB_{pol}/B_\phi}{\partial(R,Z)}(X_{pol}(x_0,\phi_s,\phi_e),\phi_e)\,\mathcal{D}X_{pol}(x_0,\phi_s,\phi_e)$$

这个矩阵经常会用，简记作 $\mathbf{A}(\phi):=\frac{\partial\left(RB_{pol}/B_\phi\right)}{\partial(R,Z)}(X_{pol}(x_0,\phi_s,\phi),\phi)$

$$\frac{\partial}{\partial\phi_e}\mathcal{D}X_{pol}(\phi_s,\phi_e)=\mathbf{A}(\phi_e)\,\mathcal{D}X_{pol}(\phi_s,\phi_e)$$

# Field line tracing sensitivity to the initial condition

## 磁力线追踪对起始点的敏感性

磁力线追踪中微元体积/面积和场的散度有什么关联？

$$\dot{\boldsymbol{x}} = \boldsymbol{B}(\boldsymbol{x})$$

$$\left|\mathcal{D}\boldsymbol{X}(\boldsymbol{x}_0, t)\right| = e^{\int_0^t \mathrm{tr}\,\nabla \boldsymbol{B}(\boldsymbol{X}(\boldsymbol{x}_0,\tau))\mathrm{d}\tau} = e^{\int_0^t \nabla\cdot\boldsymbol{B}(\boldsymbol{X}(\boldsymbol{x}_0,\tau))\mathrm{d}\tau}$$

$$\left|\mathcal{D}\boldsymbol{X}_{pol}(\phi_s, \phi_e)\right| = \exp\left(\int_{\phi_s}^{\phi_e} \frac{R(\nabla\cdot\boldsymbol{B})}{B_\phi}\mathrm{d}\phi\right)\frac{B_\phi|_{\phi_s}}{B_\phi|_{\phi_e}}$$

$$\frac{\partial}{\partial\phi_e}\boldsymbol{X}_{pol}(\boldsymbol{x}_0,\phi_s,\phi_e) = \frac{R\boldsymbol{B}_{pol}}{B_\phi}\left(\boldsymbol{X}_{pol}(\boldsymbol{x}_0,\phi_s,\phi_e),\phi_e\right)$$

- 对初值的导数记作 $\mathcal{D}\boldsymbol{X}_{pol}(\boldsymbol{x}_0,t) := \partial\boldsymbol{X}_{pol}(\boldsymbol{x}_0,t)/\partial(x_{0R},x_{0Z})$

套一下链式法则，就得到了

$$\frac{\partial}{\partial\phi_e}\mathcal{D}\boldsymbol{X}_{pol}(\boldsymbol{x}_0,\phi_s,\phi_e) = \frac{\partial R\boldsymbol{B}_{pol}/B_\phi}{\partial(R,Z)}(\boldsymbol{X}_{pol}(\boldsymbol{x}_0,\phi_s,\phi_e),\phi_e)\,\mathcal{D}\boldsymbol{X}_{pol}(\boldsymbol{x}_0,\phi_s,\phi_e)$$

这个矩阵经常会用，简记作 $\mathbf{A}(\phi) := \frac{\partial\left(R\boldsymbol{B}_{pol}/B_\phi\right)}{\partial(R,Z)}(\boldsymbol{X}_{pol}(\boldsymbol{x}_0,\phi_s,\phi),\phi)$

$$\frac{\partial}{\partial\phi_e}\mathcal{D}\boldsymbol{X}_{pol}(\phi_s,\phi_e) = \mathbf{A}(\phi_e)\,\mathcal{D}\boldsymbol{X}_{pol}(\phi_s,\phi_e)$$

# Field line tracing sensitivity to the initial condition

磁力线追踪对起始点的敏感性

- $\mathcal{DP}^{\pm m}$ 的环上演化

$$\frac{\mathrm{d}}{\mathrm{d}\phi}\mathcal{DP}^{\pm m}(\phi) = [\mathbf{A}(\phi), \mathcal{DP}^{\pm m}(\phi)]$$

- 对环而言，$\phi_e = \phi_s \pm 2m\pi$ 的时候 $X_{\mathrm{pol}}$ 打回原点
- 为什么用 $m$ 符号？

  一个有理面上的环，如果有理面安全因子 $q = \frac{m}{n} = 1/\iota$，它会在环向上转 $m$ 圈，极向上转 $n$ 圈回到出发点。

$$\frac{\partial}{\partial\phi_e}\mathcal{D}X_{pol}(\phi_s,\phi_e) = \mathbf{A}(\phi_e)\,\mathcal{D}X_{pol}(\phi_s,\phi_e)$$

# Evolution of the eigenvectors of $\mathcal{DP}^{\pm m}$ along a cycle

双曲环上 $\mathcal{DP}^{\pm m}$ 的特征方向的演化

- $\mathcal{DP}^{\pm m}$ 的环上演化

$$\frac{\mathrm{d}}{\mathrm{d}\phi}\mathcal{DP}^{\pm m}(\phi) = [\mathbf{A}(\phi), \mathcal{DP}^{\pm m}(\phi)]$$

- $\mathcal{DP}^{\pm m}$ 特征向量的环上演化

$$\mathbf{\Theta}' = \left(\begin{bmatrix} & -1 \\ 1 & \end{bmatrix}\mathbf{V}\mathbf{\Lambda} - \mathcal{DP}^{\pm m}\begin{bmatrix} & -1 \\ 1 & \end{bmatrix}\mathbf{V}\right)^{-1}(\mathcal{DP}^{\pm m})'\mathbf{V}$$

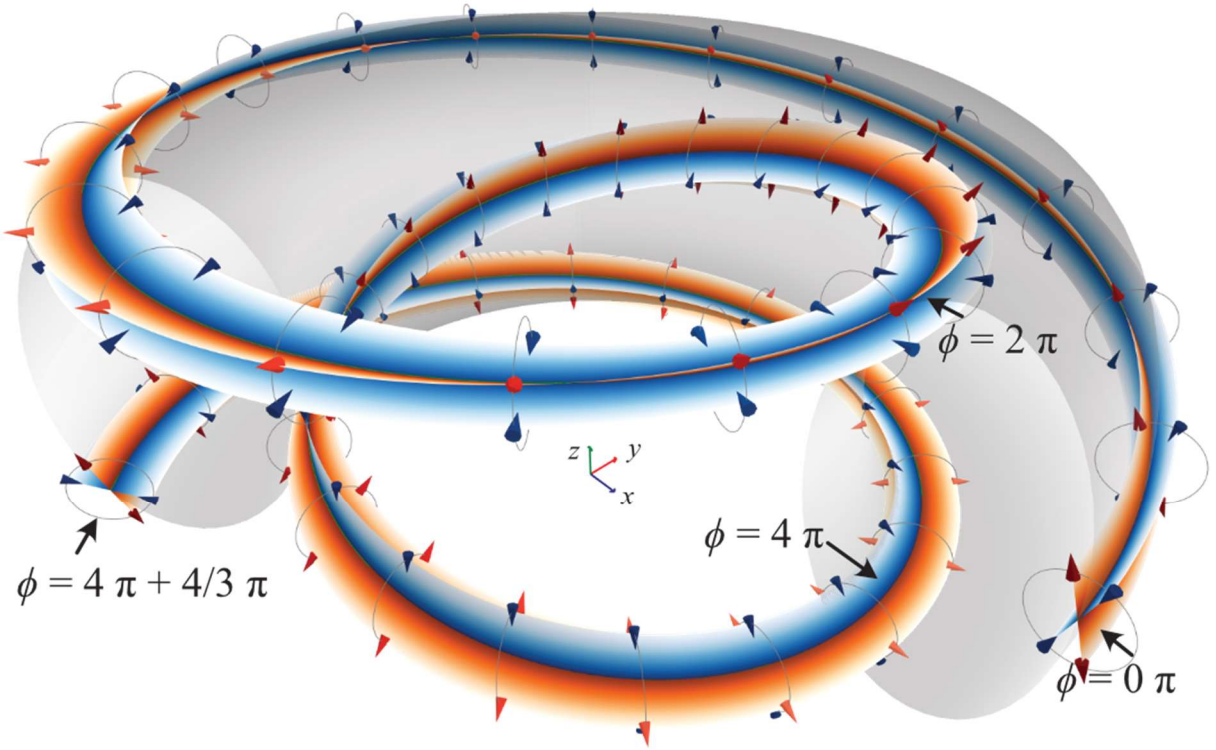


两者在数学上是等价的，数值实验证实了两者等价

- 但特征向量的演化在两个特征方向很靠近的时候数值上很麻烦，建议用前者直接演化 $\mathcal{DP}^{\pm m}$ 之后再梳理特征方向

# Classification of cycles

## 环的分类

- $\mathcal{D}P^{\pm m}$ 的环上演化方程的交换子形式决定了环上的 $\mathcal{D}P^{\pm m}$ 特征值不变，使得依据 $\mathcal{D}P^{\pm m}$ 的特征值对环分类成为可能。
  - 椭圆环 **elliptic cycles** 对应 O 点
  - 抛物环 **parabolic cycles** 对应有理面上的环
  - 双曲环 **hyperbolic cycles** 对应 X 点
- 二维自治动力系统有成熟的划分。散度为零的向量场诱导的 **Poincaré** 映射最后只能落在中间 y 轴上。

- 环上演化方程可以推广至 $n$ 维，使得**任意有限维**自治连续动力系统都可以适用，不要求散度为零。

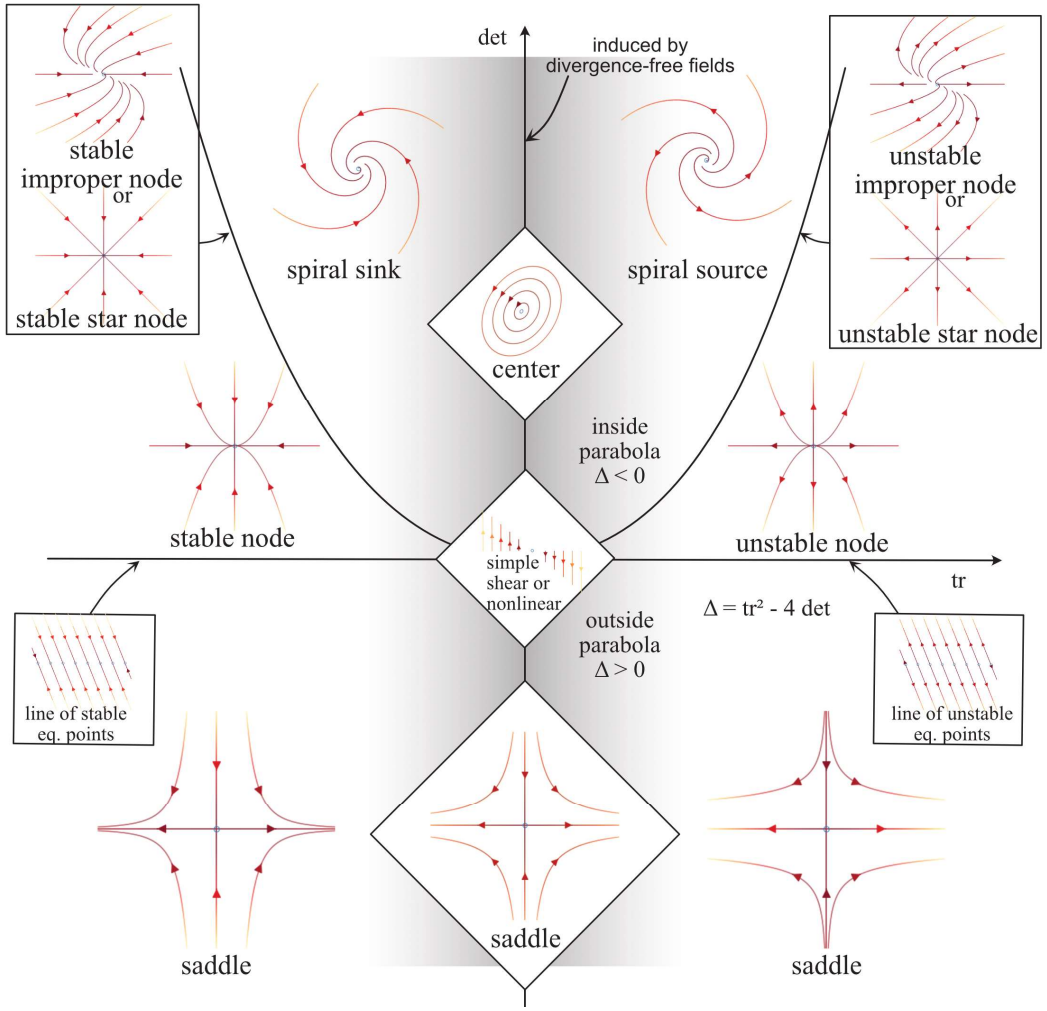


Fig. 二维自治动力系统根据平衡点的 Jacobian 的经典分类

# Classification of cycles

## 环的分类

### DEFINITION 定义

$\mathcal{D}P^m$特征值在不在 $\mathbb{S}$ 上

cycles of 3D flows

- hyperbolic — X-环
  - saddle
    - non-Möbiusian — if both $\lambda$ positive
    - Möbiusian — if both $\lambda$ negative
  - sinking — if both $\lambda$ inside $\mathbb{S}$
  - sourcing — if both $\lambda$ outside $\mathbb{S}$
- partially hyperbolic (but not hyperbolic) — if one eigenvalue $\lambda = 1$ or $-1$, while the other $\lambda \in \mathbb{R} \setminus \{1, -1\}$
- non-hyperbolic — 0-环
  - elliptic — if both $\lambda$ on $\mathbb{S}$ but $\neq \pm 1$
  - parabolic — if both $\lambda = 1$ or $-1$

对磁场不可能有这样的环，其他的向量场可能可以

有理面上的环

0-环上的 $\mathcal{D}X_{\mathrm{pol}}$ 的两个特征值会以平均下来为 $\iota$ 的速度在复平面上的标准圆 $\mathbb{S}$ 旋转，一正转一反转。

The two eigenvalues of $\mathcal{D}X_{\mathrm{pol}}$ rotate along $\mathbb{S} \subset \mathbb{C}$ with an average speed of $\iota$, clockwise and counter-clockwise, respectively.

# Invariant manifold growth formula

## 不变流形生长公式

- 鞍环的稳定和不稳定流形是无尽延伸结构，不宜用磁面坐标$(\theta,\phi)$，改用$(s,\phi)$。s是R-Z截面切掉这一流形的曲线的长度，$\phi$就是正常的柱坐标。
- 接着用磁力线追踪方程为基础，分析一下各微元关系即可。

流形生长公式不要求**散度为零**，其他向量场满足条件也可以用，例如$\boldsymbol{E},\boldsymbol{j},\boldsymbol{v}$。

• Fig. 流形示意图（假设下单零位型）

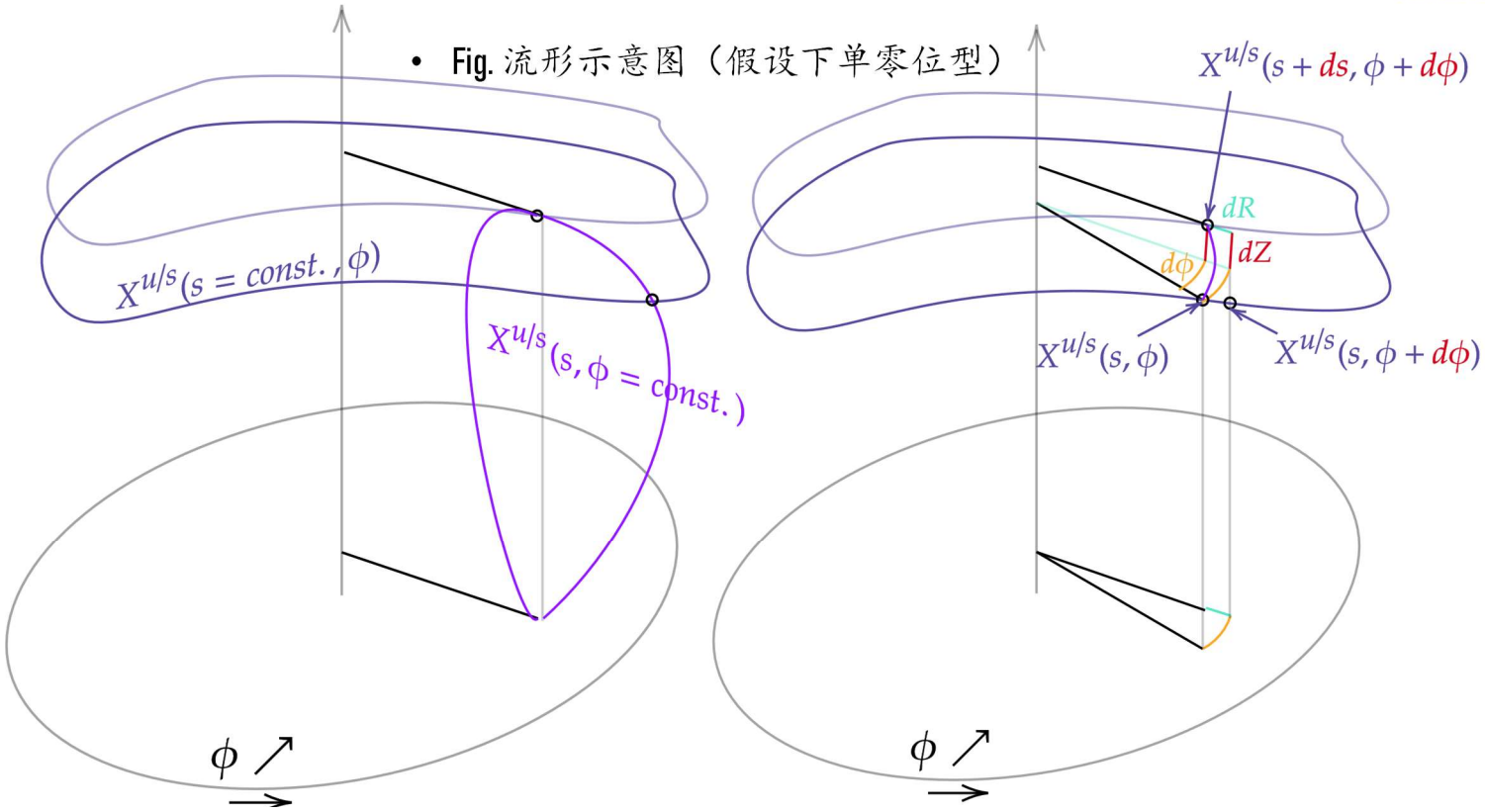


$$\frac{\partial \boldsymbol{X}^{u/s}}{\partial s}(s,\phi)=\frac{\frac{R\boldsymbol{B}_{pol}}{B_\phi}(\boldsymbol{X}^{u/s},\phi)-\frac{\partial \boldsymbol{X}^{u/s}}{\partial \phi}(s,\phi)}{\pm\left\|\frac{R\boldsymbol{B}_{pol}}{B_\phi}(\boldsymbol{X}^{u/s},\phi)-\frac{\partial \boldsymbol{X}^{u/s}}{\partial \phi}(s,\phi)\right\|_2}$$

这个分母是ds/dϕ，所以如果磁力线随$\phi$增大远离X环，±取+，否则取−。

# Invariant manifold growth formula abbreviated

## 不变流形生长公式的简写

$$\frac{\partial \boldsymbol{X}^{u/s}}{\partial s}(s,\phi) = \frac{\frac{R\boldsymbol{B}_{pol}}{B_\phi}(\boldsymbol{X}^{u/s},\phi) - \frac{\partial \boldsymbol{X}^{u/s}}{\partial \phi}(s,\phi)}{\pm\left\|\frac{R\boldsymbol{B}_{pol}}{B_\phi}(\boldsymbol{X}^{u/s},\phi) - \frac{\partial \boldsymbol{X}^{u/s}}{\partial \phi}(s,\phi)\right\|_2}$$

$$\frac{\partial \boldsymbol{X}^{u/s}}{\partial s} = \frac{\frac{R\boldsymbol{B}_{pol}}{B_\phi} - \frac{\partial \boldsymbol{X}^{u/s}}{\partial \phi}}{\pm\left\|\frac{R\boldsymbol{B}_{pol}}{B_\phi} - \frac{\partial \boldsymbol{X}^{u/s}}{\partial \phi}\right\|_2}$$

$$\frac{\partial \boldsymbol{X}^{u/s}}{\partial s} = \frac{R\boldsymbol{B}_{pol}}{B_\phi} - \frac{\partial \boldsymbol{X}^{u/s}}{\partial \phi} \quad /\pm\|\cdots\|$$

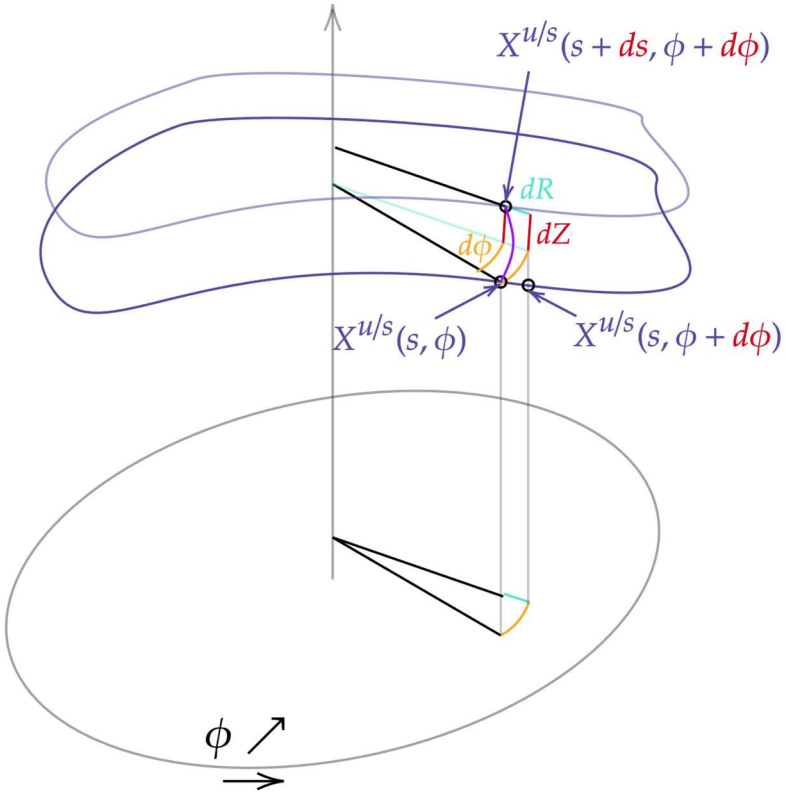

# 1D invariant manifold growth formula

一维不变流形生长公式

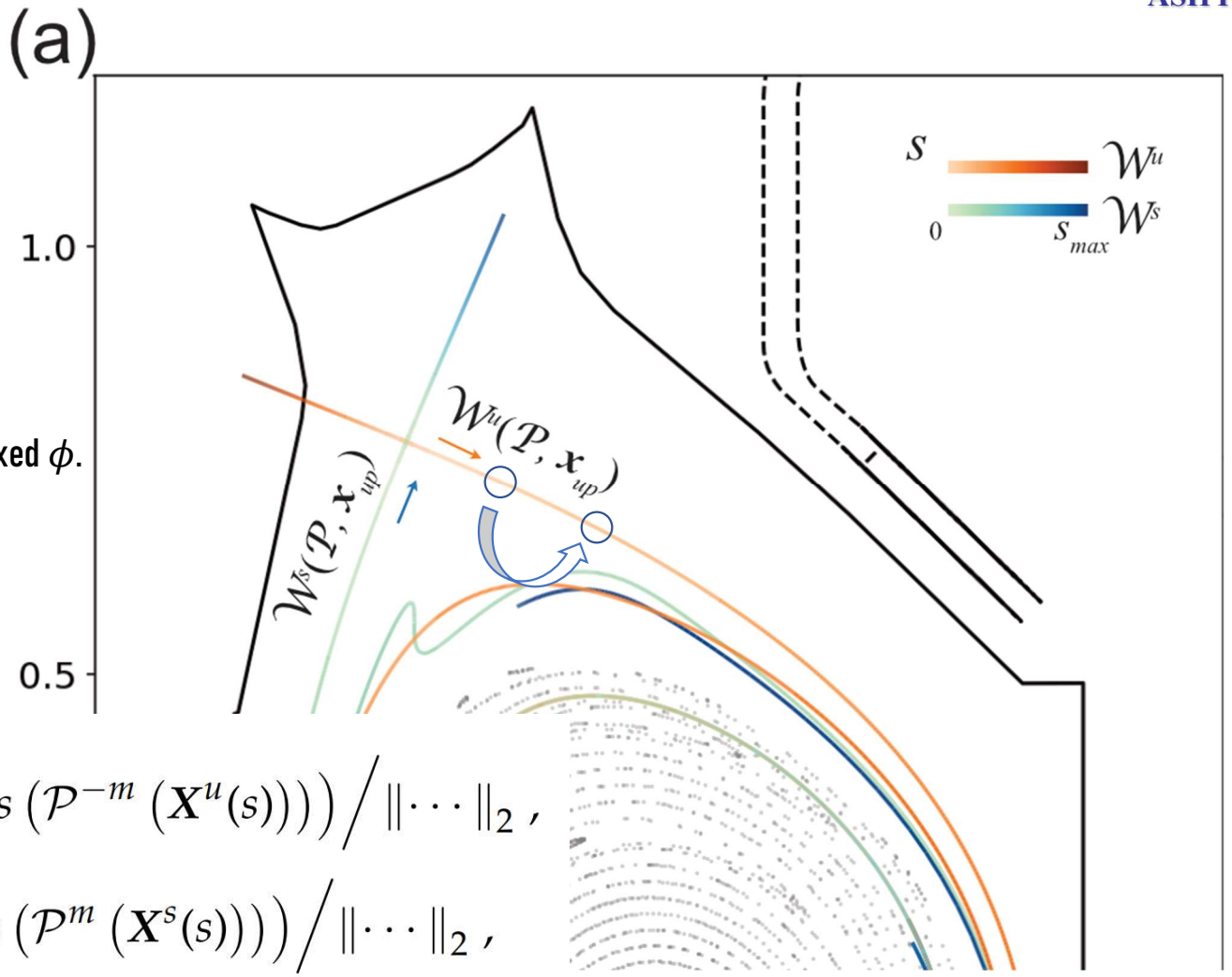


- If the only known is limited to one section $\phi$,
  i.e. we only know $\mathcal{P}^m(\boldsymbol{x}_0, \phi)$ and $\mathcal{D}\mathcal{P}^m(\boldsymbol{x}_0, \phi)$ at a fixed $\phi$.
- 如果只知道在一个截面的信息，
  换言之，只知道当 $\phi$ 在一个角时的
  $\mathcal{P}^m(\boldsymbol{x}_0, \phi)$ 和 $\mathcal{D}\mathcal{P}^m(\boldsymbol{x}_0, \phi)$

$$\frac{\mathrm{d}X^u(s)}{\mathrm{d}s} = \mathcal{D}\mathcal{P}^m\left(\mathcal{P}^{-m}\left(X^u(s)\right)\right) \cdot \frac{\mathrm{d}X^u}{\mathrm{d}s}\left(s\left(\mathcal{P}^{-m}\left(X^u(s)\right)\right)\right) \Big/ \|\cdots\|_2 ,$$

$$\frac{\mathrm{d}X^s(s)}{\mathrm{d}s} = \mathcal{D}\mathcal{P}^{-m}\left(\mathcal{P}^{m}\left(X^s(s)\right)\right) \cdot \frac{\mathrm{d}X^s}{\mathrm{d}s}\left(s\left(\mathcal{P}^{m}\left(X^s(s)\right)\right)\right) \Big/ \|\cdots\|_2 ,$$

- 类似地，该公式也可以用在闭合的有理和无理面上。Similarly, this formula can also apply to (ir)rational flux surfaces.

# Invariant manifold growth formula in axisymmetric vector field

## 不变流形生长公式于轴对称的场中

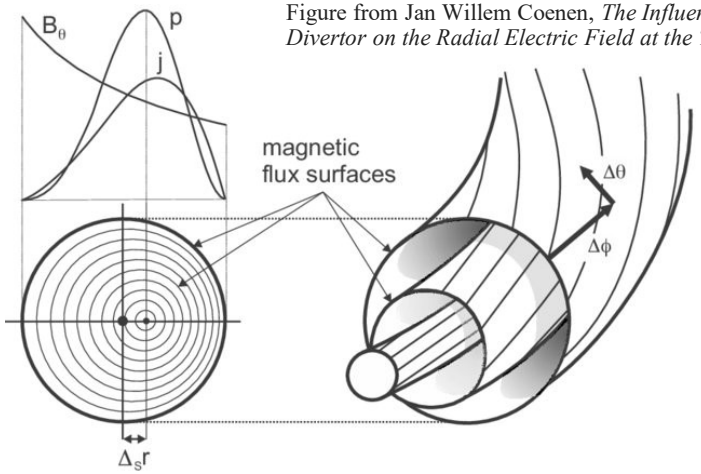


Figure from Jan Willem Coenen, *The Influence of the Dynamic Ergodic Divertor on the Radial Electric Field at the Tokamak TEXTOR* [D] 2009

$$\frac{\partial \boldsymbol{X}^{u/s}}{\partial s} = \frac{R\boldsymbol{B}_{pol}}{B_\phi} - \frac{\partial \boldsymbol{X}^{u/s}}{\partial \phi} \Big/ \pm \|\cdots\|$$

取一个非不变的“环”，

譬如取 $R_c(\phi), Z_c(\phi)$ 都是常数。

Pick a non-invariant “cycle”,

e.g. a cycle with $R_c(\phi), Z_c(\phi)$ constant.

$$\frac{\partial \boldsymbol{X}^{u/s}}{\partial s} = \left( \frac{R\boldsymbol{B}_{pol}}{B_\phi} - \cancel{\frac{\partial \boldsymbol{X}^{u/s}}{\partial \phi}}^{\,0} \right) \Big/ \pm \|\cdots\|_2$$

$$\frac{\partial \boldsymbol{X}^{u}}{\partial s} = \hat{\boldsymbol{b}}_{\mathrm{pol}} \quad \text{or} \quad -\hat{\boldsymbol{b}}_{\mathrm{pol}}$$

# Homoclinic/heteroclinic connection/intersection

## 同宿/异宿 连接/相交

最外闭合磁面各自从 X 点伸出的流形在轴对称场下是重合的，称为同宿连接；在 RMP 扰动场下它们不再重合，称之为同宿相交。

| | |
|---|---|
| 同宿连接/相交 | Homoclinic connection/intersection |
| 同宿轨/迹 | Homoclinic trajectory/orbit |
| 异宿连接/相交 | Heteroclinic connection/intersection |
| 异宿轨/迹 | Heteroclinic trajectory/orbit |

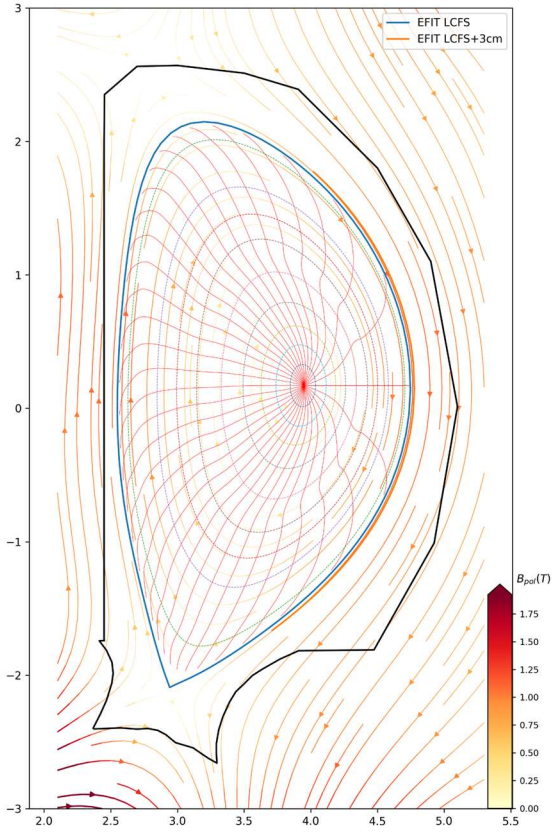


Fig. BEST $(s, \theta^*, \phi)$ mesh.

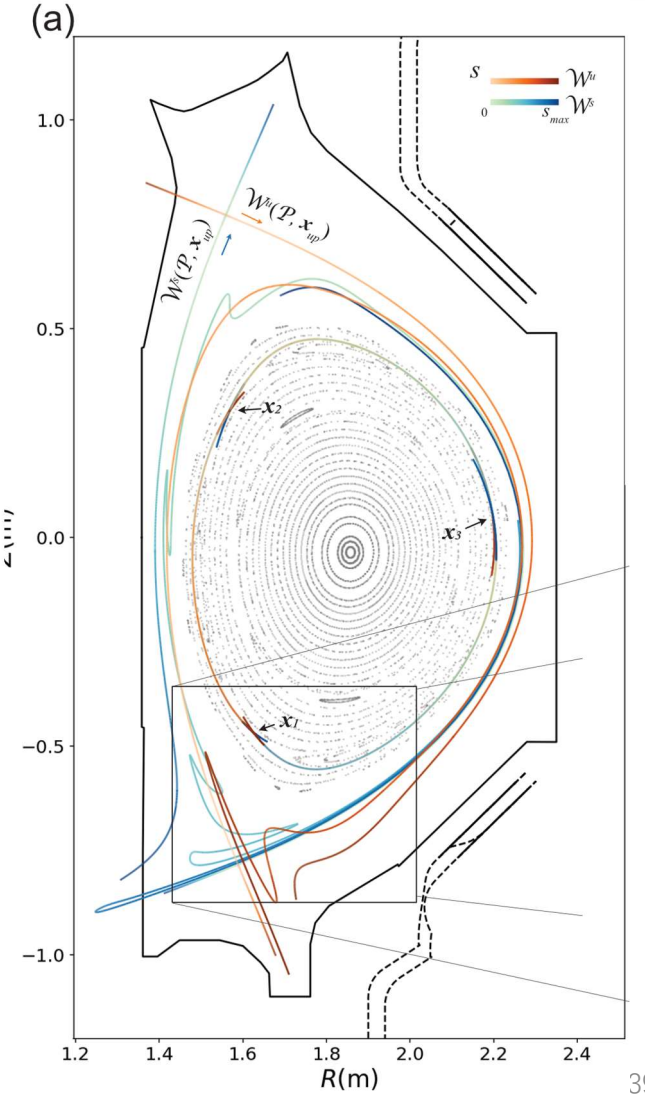


Fig. RMP 下 EAST #103950 @ 3500ms

# Homoclinic/heteroclinic connection/intersection

## 同宿/异宿 连接/相交

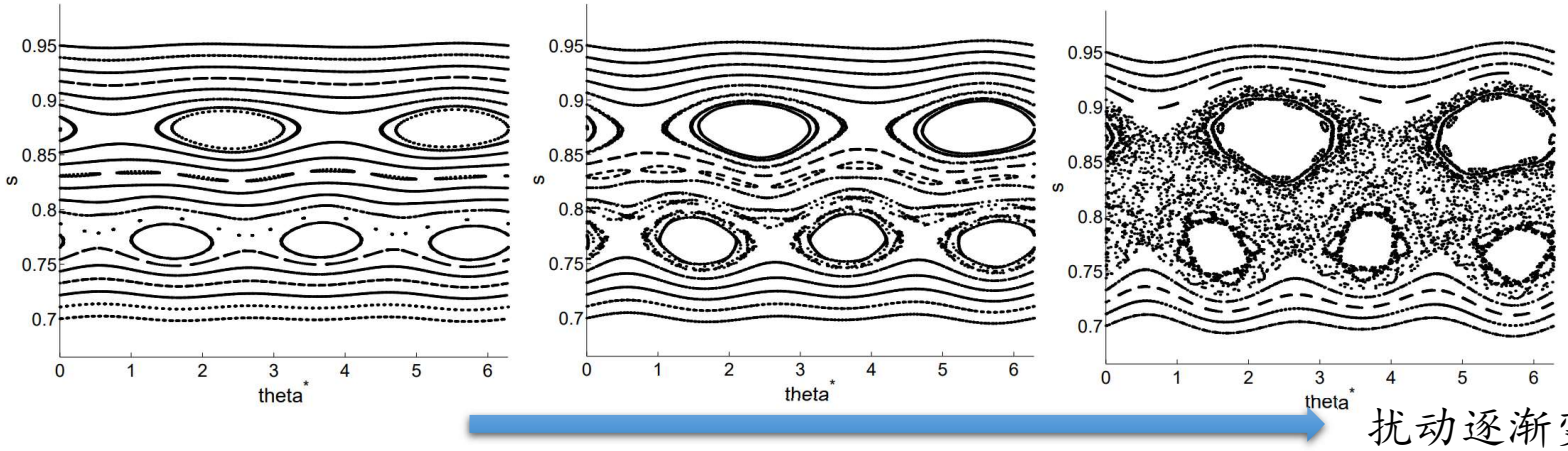


同宿连接/相交 Homoclinic connection/intersection

同宿轨/迹 Homoclinic trajectory/orbit

异宿连接/相交 **Heteroclinic connection/intersection**

异宿轨/迹 **Heteroclinic trajectory/orbit**

异宿连接可以发生在双零位形，
异宿相交可以发生在两磁岛链有所重合的时候。

# 目录 Outline

- 背景介绍
  - 嵌套闭合磁面假设
  - 学科分野
  - Poincaré-Hopf 定理
  - Poincaré-Birkhoff 定理
  - 三维磁拓扑相关的实验和模拟研究
  - KAM 定理
  - 现代的共振磁扰动磁谱分析方法
- 流形生长
  - 不变流形的定义
  - 磁力线对初值的敏感性$\mathcal{D}\boldsymbol{X}_{\mathrm{pol}}$
  - $\mathcal{D}\mathcal{P}^{\pm m}$ 在环上的演化和环的分类
  - 生长流形的经典方法和新方法
  - 不变流形的样例演示及解析的例子
- 回顾与展望
  - 边界磁拓扑
  - 最外闭合磁面的确定
  - 拓扑控制

# Classical method to grow manifolds

## 生长流形的经典方法

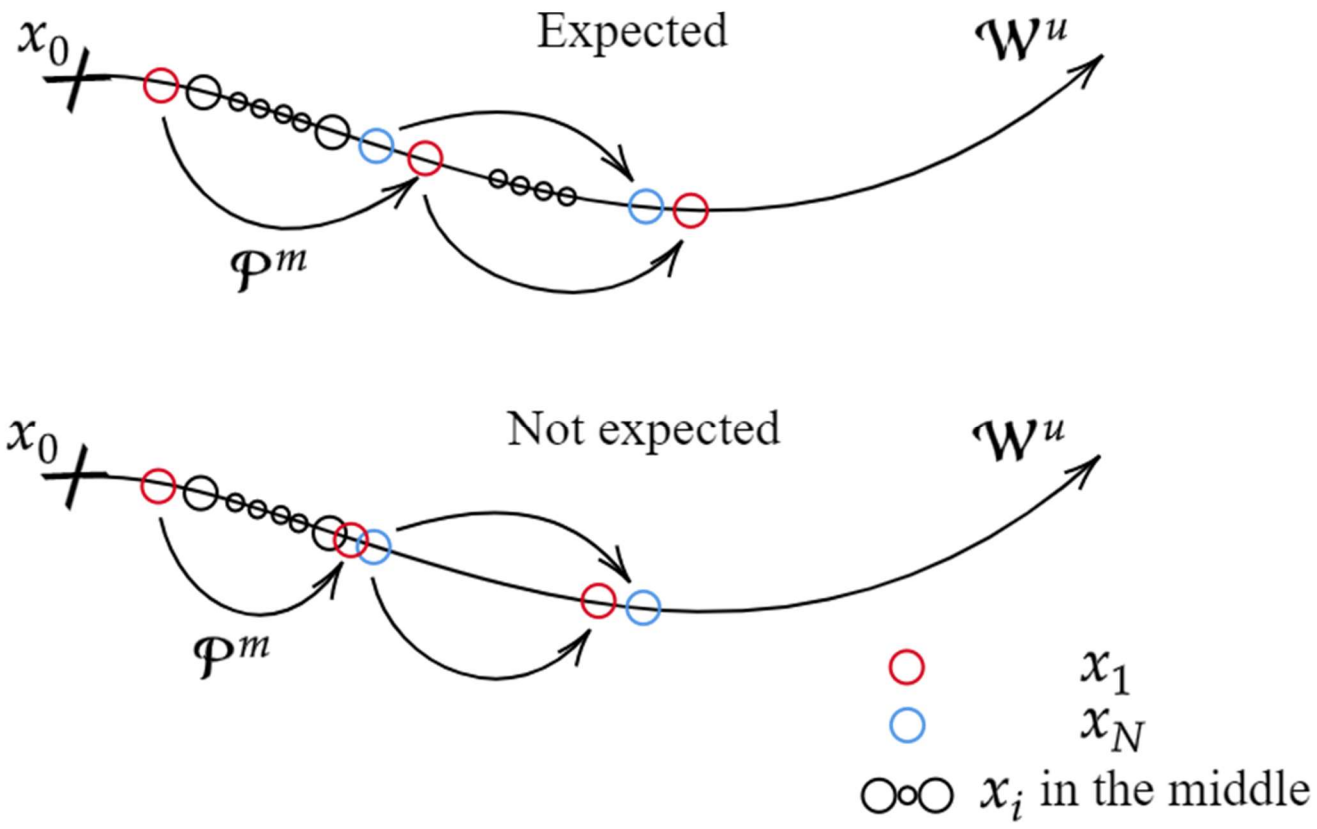


**Untangled**

没有纠缠在一起

**Tangled**

纠缠在一起

# Classical method to grow manifolds

## 生长流形的经典方法

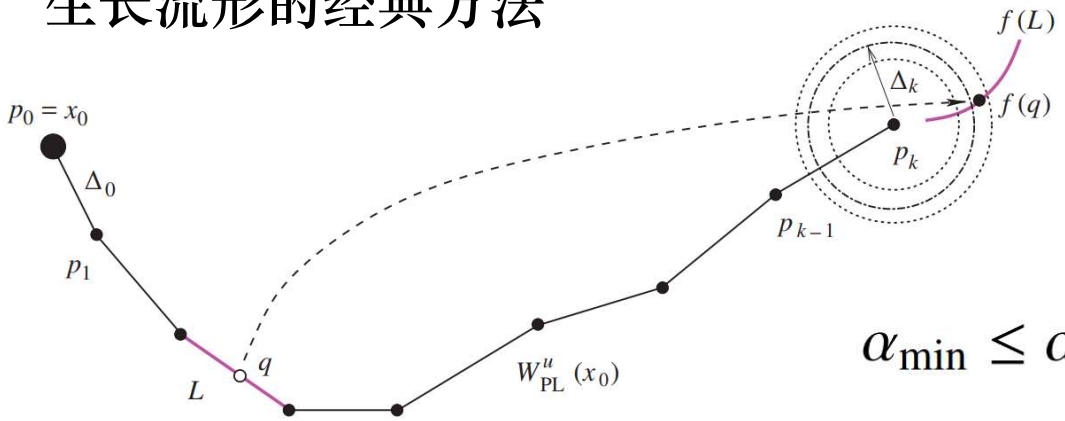


Fig. Growing the unstable manifold [1,2,4]

$$\alpha_{\min} \le \alpha_k \le \alpha_{\max} \quad \text{and} \quad (\Delta\alpha)_{\min} \le \Delta_k \alpha_k \le (\Delta\alpha)_{\max}$$

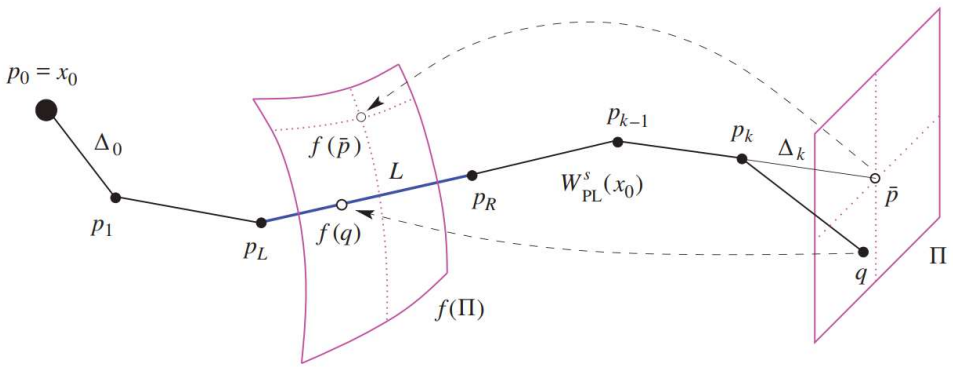


Fig. Growing the stable manifold [3,4]

传统的数值流形生长方法（不断迭代试探）对环几何显得十分多余，

因为它们只研究**孤立的单个映射 (map)**，

而不同 $\phi$ 角截面的 **Poincare** 映射是**相互之间有关联的**。

[1] Krauskopf, B., and Osinga, H. M. 1998. Globalizing two-dimensional unstable manifolds of maps. *Internat. J. Bifur. Chaos Appl. Sci. Engrg.*, **8**(3), 483–503.
[2] Krauskopf, B., and Osinga, H. M. 1998. Growing 1D and quasi-2D unstable manifolds of maps. *J. Comput. Phys.*, **146**(1), 404–419.
[3] England, J. P., Krauskopf, B., and Osinga, H. M. 2004. Computing one-dimensional stable manifolds and stable sets of planar maps without the inverse. *SIAM J. Appl. Dyn. Syst.*, **3**(2), 161–190.
[4] Figures drawn in Yuri Kuznetsov, *Numerical bifurcation of maps: From theory to software*. 2020

# Our method to grow manifolds

生长流形的新方法

在 $x_0$ 的小领域周围 Around a small neighborhood of $x_0$

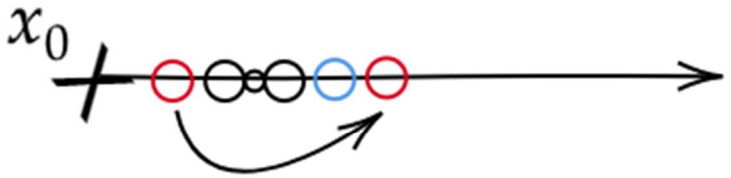


$$\mathcal{P}^m(x_1) - x_0 \approx \lambda_u \cdot (x_1 - x_0)$$

要保持点列依然是有序的，
我们只需要使 To keep the sequence ordered, *i.e.* $|\mathcal{P}^m(x_1) - x_0| > |x_N - x_0|$,
one simply needs to let $|x_N - x_0| < \lambda_u |x_1 - x_0|$.

# A realistic numeric example on EAST

现实中 EAST 上的数值例子

$$\mathcal{W}^{u/s}(\boldsymbol{B},\gamma) = \bigcup_{\phi\in[0,2m\pi)} \left\{ \boldsymbol{x}(R,Z,\phi) \in M \mid (R,Z) \in \mathcal{W}^{u/s}(\mathcal{P}^m(\phi), \boldsymbol{x}(\phi)) \right\}$$

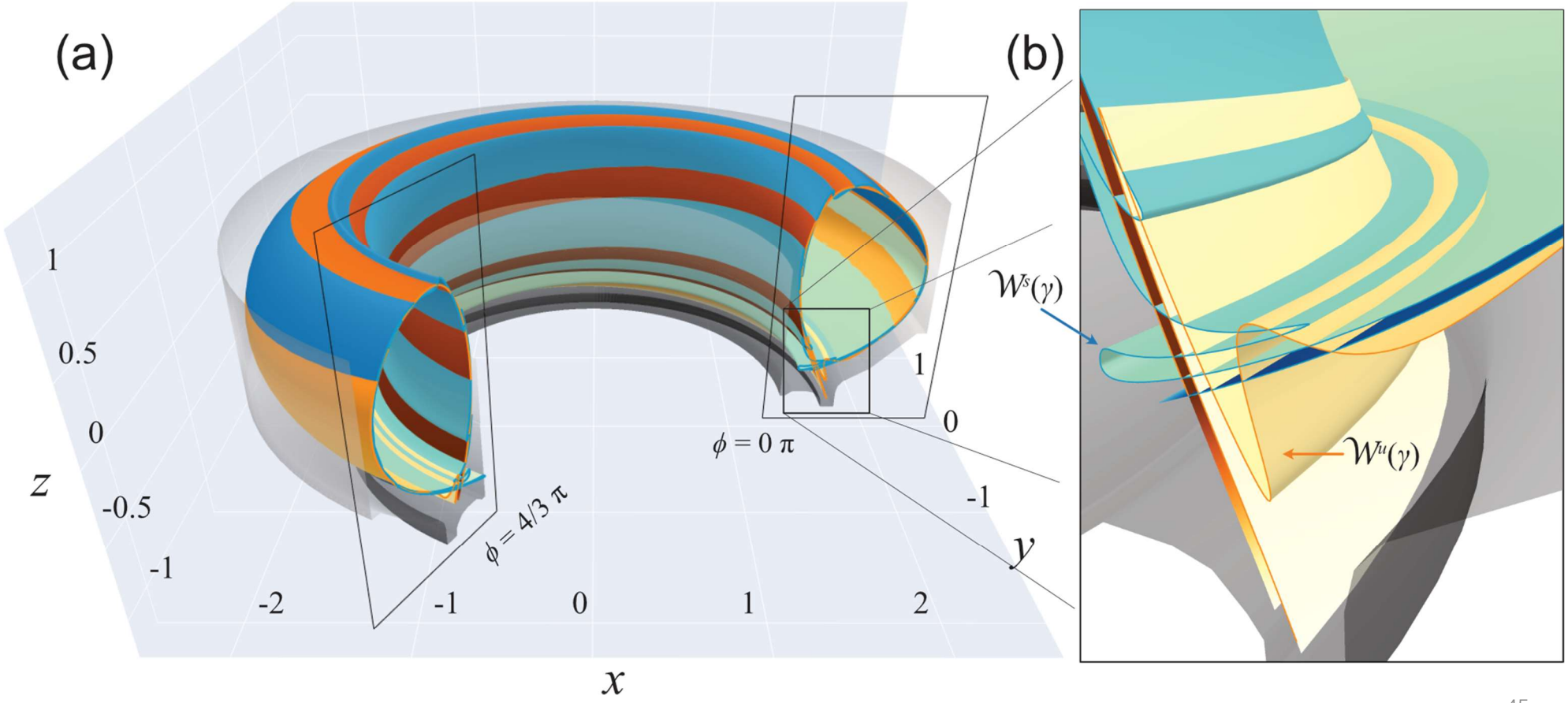


Fig. RMP 下 EAST #103950 @ 3500ms

# A realistic numeric example on EAST

现实中 EAST 上的数值例子

$$\mathcal{W}^{u/s}(\boldsymbol{B},\gamma) = \bigcup_{\phi\in[0,2m\pi)} \left\{ \boldsymbol{x}(R,Z,\phi) \in M \mid (R,Z) \in \mathcal{W}^{u/s}(\mathcal{P}^m(\phi),\boldsymbol{x}(\phi)) \right\}$$

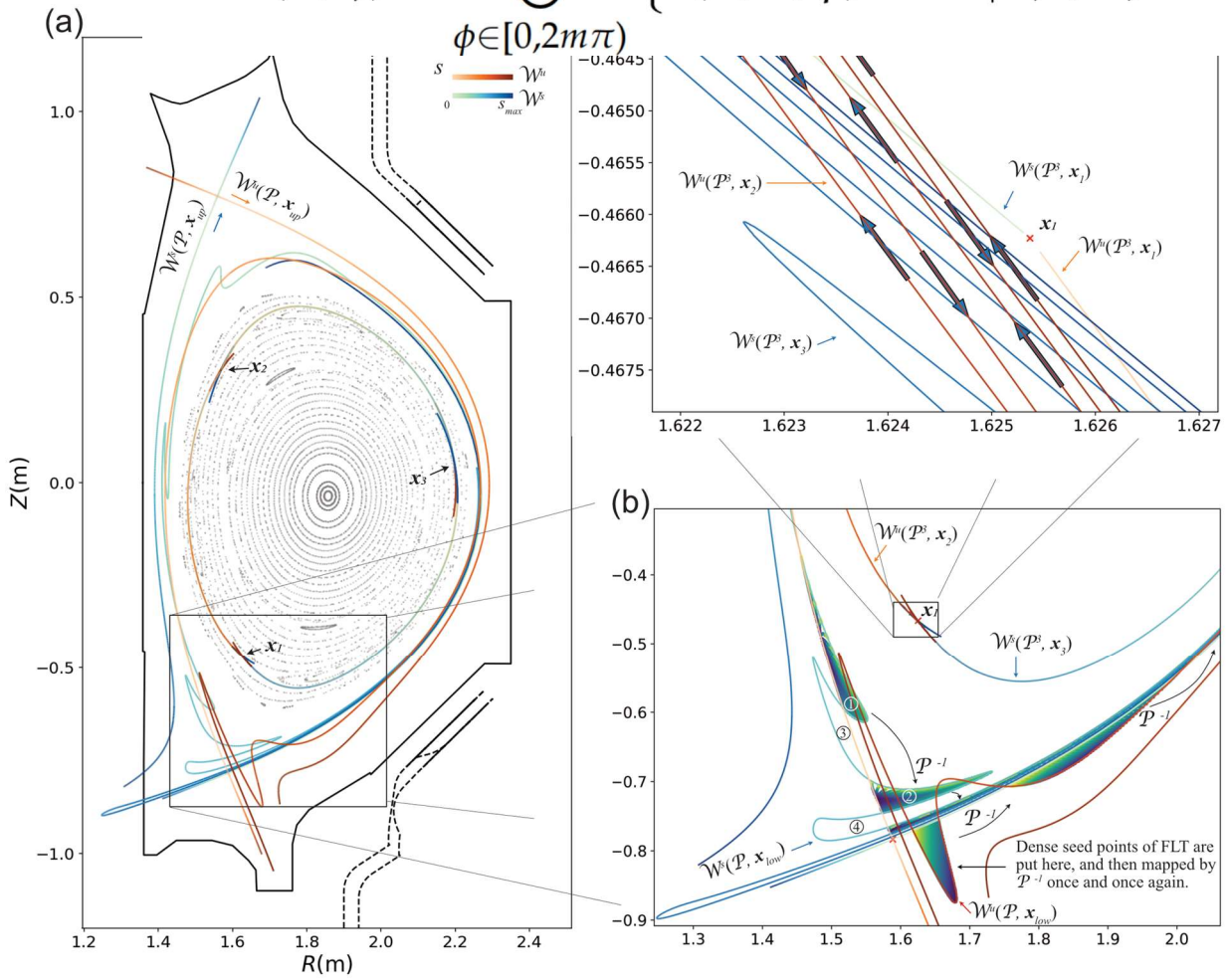


Fig. RMP 下 EAST #103950 @ 3500ms, $\phi = 0$ rad

# A realistic numeric example on EAST

## 现实中 EAST 上的数值例子

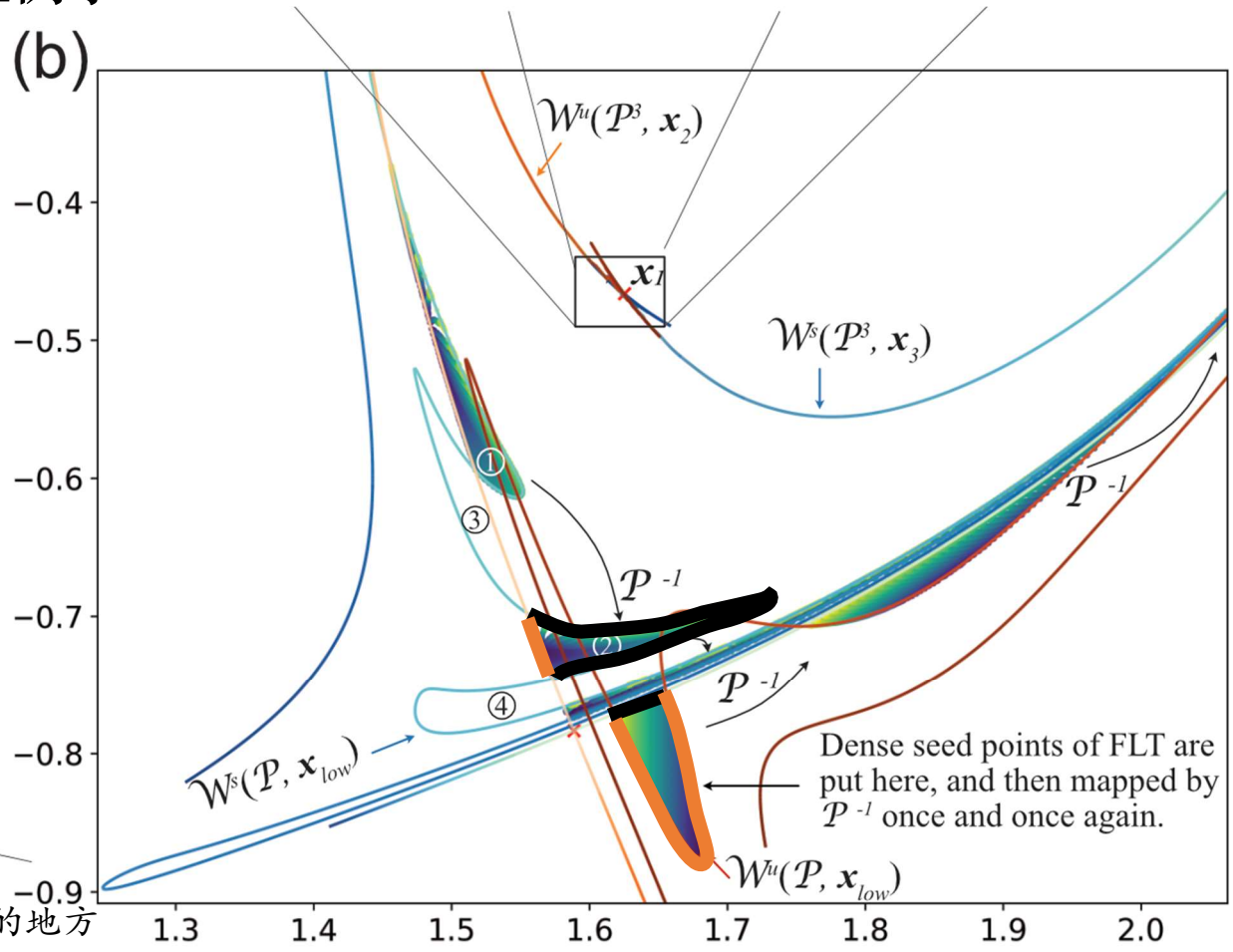


- 偏滤器
  - 小心热负荷打到未设计好的地方
  - 热负荷沉积区升至二维，不必局限在一维
- 诊断会关心等离子体边界 $n$ 剖面可能非单调

# A Möbiusian/non-Möbiusian cycle

莫比乌斯环/非莫比乌斯环

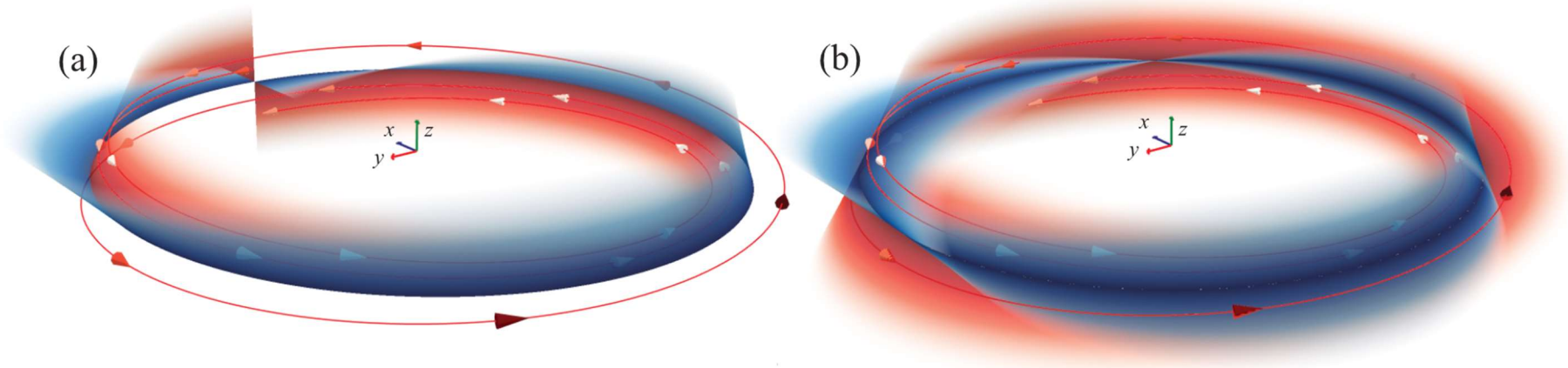


$$\boldsymbol{X}_{pol}(\phi) = \begin{cases} |\lambda_u|^{\phi/2m\pi} \begin{bmatrix} \cos\theta_u(\phi) \\ \sin\theta_u(\phi) \end{bmatrix} + \begin{bmatrix} R_0 \\ Z_0 \end{bmatrix}, & \textit{(for unstable trajectories)} \\ |\lambda_s|^{\phi/2m\pi} \begin{bmatrix} \cos\theta_s(\phi) \\ \sin\theta_s(\phi) \end{bmatrix} + \begin{bmatrix} R_0 \\ Z_0 \end{bmatrix}, & \textit{(for stable trajectories)} \end{cases}$$

- 已有期望的轨迹，如何构造其场？

**How to construct a field for a desired cycle?**

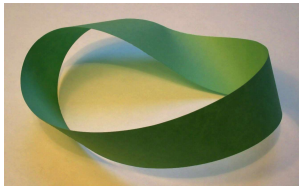

- 注意我们构造的是莫比乌斯环，而不是传统的莫比乌斯条带

**Note that what we construct is a Möbiusian cycle instead of a classical Möbius strip.**

# A Möbiusian/non-Möbiusian cycle

## 莫比乌斯环/非莫比乌斯环

$$X_{pol}(\phi) = \begin{cases} |\lambda_u|^{\phi/2m\pi} \begin{bmatrix} \cos\theta_u(\phi) \\ \sin\theta_u(\phi) \end{bmatrix} + \begin{bmatrix} R_0 \\ Z_0 \end{bmatrix}, & \textit{(for unstable trajectories)} \\ |\lambda_s|^{\phi/2m\pi} \begin{bmatrix} \cos\theta_s(\phi) \\ \sin\theta_s(\phi) \end{bmatrix} + \begin{bmatrix} R_0 \\ Z_0 \end{bmatrix}, & \textit{(for stable trajectories)} \end{cases}$$

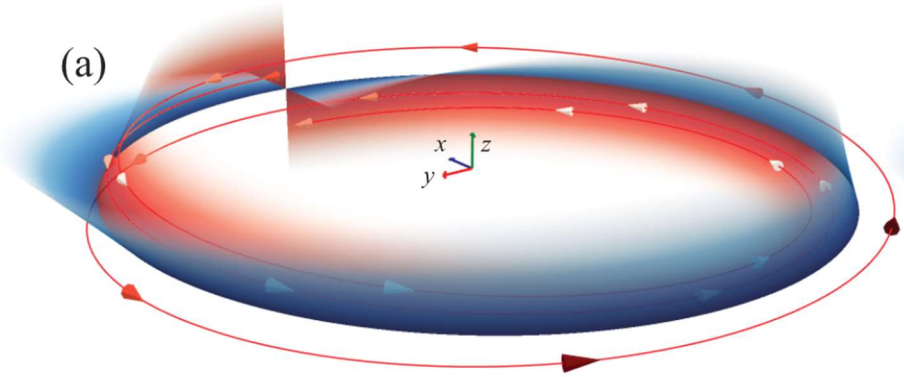


Let $\Delta X_{pol}(\phi) := X_{pol}(\phi) - [R_0, Z_0]^T$. For the unstable trajectories, $\Delta X'_{pol}(\phi)$ is

左导右不导　　左不导右导

$$\frac{\mathrm{d}}{\mathrm{d}\phi}\Delta X_{pol}(\phi) = \left(|\lambda_u|^{\phi/2m\pi}\right)' \begin{bmatrix} \cos\theta_u \\ \sin\theta_u \end{bmatrix} + |\lambda_u|^{\phi/2m\pi} \left( \begin{bmatrix} \cos\theta_u \\ \sin\theta_u \end{bmatrix} \right)'$$

$$= |\lambda_u|^{\phi/2m\pi} \begin{bmatrix} \frac{\ln|\lambda_u|}{2m\pi} & -\theta'_u \\ \theta'_u & \frac{\ln|\lambda_u|}{2m\pi} \end{bmatrix} \begin{bmatrix} \cos\theta_u \\ \sin\theta_u \end{bmatrix} = \begin{bmatrix} \frac{\ln|\lambda_u|}{2m\pi} & -\theta'_u \\ \theta'_u & \frac{\ln|\lambda_u|}{2m\pi} \end{bmatrix} \Delta X_{pol}(\phi)$$

$$= \begin{bmatrix} \frac{\ln|\lambda_u|}{2m\pi} & \\ & \frac{\ln|\lambda_u|}{2m\pi} \end{bmatrix} \Delta X_{pol}(\phi) + \begin{bmatrix} & -\theta'_u \\ \theta'_u & \end{bmatrix} \Delta X_{pol}(\phi).$$

磁力线追踪方程在环周围展开　$\frac{\partial}{\partial\phi_e} X_{pol}(x_0, \phi_s, \phi_e) = \frac{RB_{pol}}{B_\phi}\left(X_{pol}(x_0, \phi_s, \phi_e), \phi_e\right)$

$$\Delta X'_{pol}(\phi) = \frac{\partial RB_{pol}/B_\phi}{\partial(R,Z)} \Delta X_{pol}(\phi) + \cdots$$

# An analytic dummy X-cycle

## 仿造 X 环的解析例子

$$X_{pol}(\phi) = \begin{cases} |\lambda_u|^{\phi/2m\pi} \begin{bmatrix} \cos\theta_u(\phi) \\ \sin\theta_u(\phi) \end{bmatrix} + \begin{bmatrix} R_0 \\ Z_0 \end{bmatrix}, & \textit{(for unstable trajectories)} \\ |\lambda_s|^{\phi/2m\pi} \begin{bmatrix} \cos\theta_s(\phi) \\ \sin\theta_s(\phi) \end{bmatrix} + \begin{bmatrix} R_0 \\ Z_0 \end{bmatrix}, & \textit{(for stable trajectories)} \end{cases}$$

$$R_c(\phi) = R_{ell}\cos\left(\iota\phi + \theta_0\right) + R_{ax},$$
$$Z_c(\phi) = Z_{ell}\sin\left(\iota\phi + \theta_0\right) + Z_{ax},$$

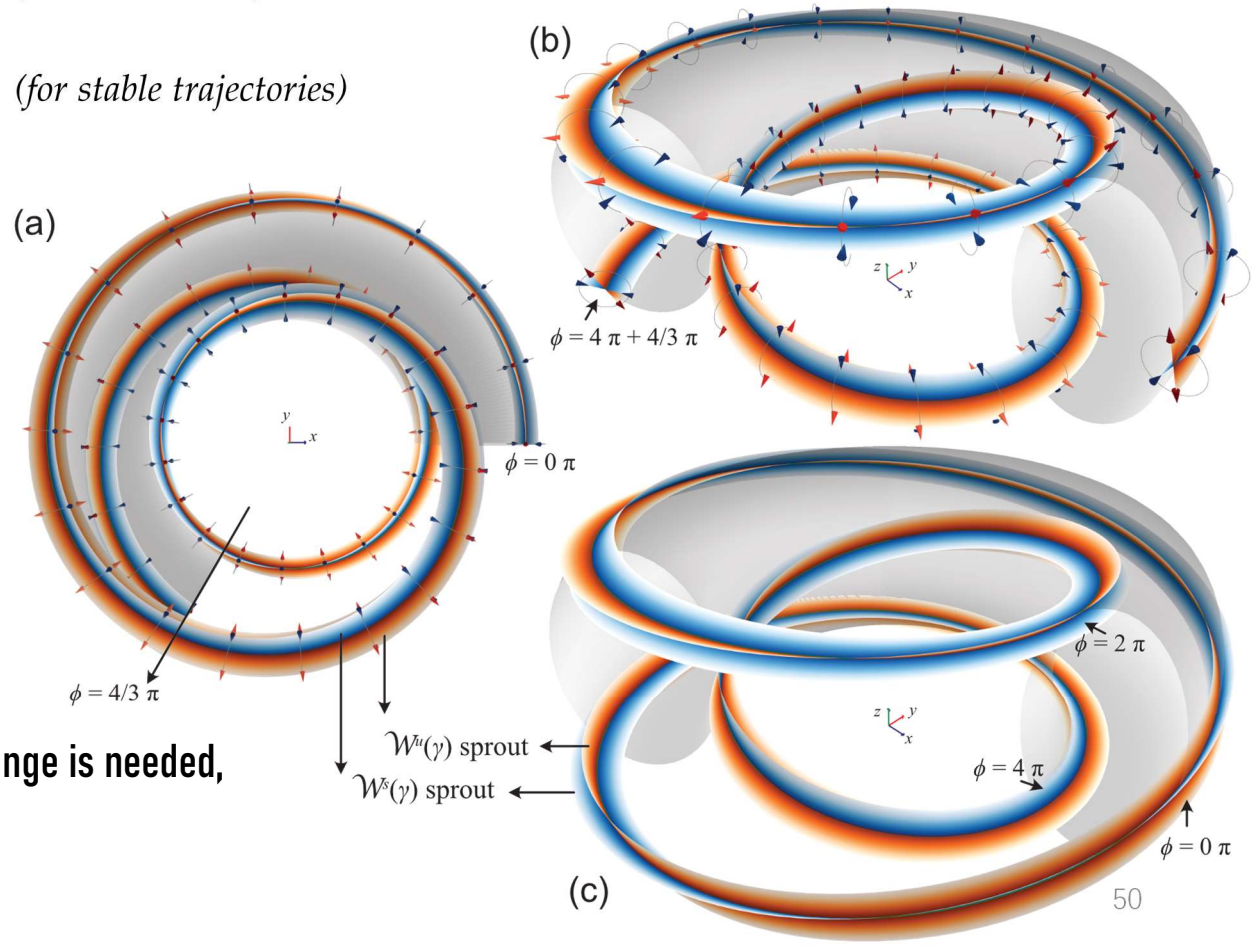


解析地仿造一 X 环，只需多加一步，

主要在于让 $R_0, Z_0$ 不再是常数。

To analytically construct an X-cycle, only one more change is needed,

that is to let $R_0, Z_0$ are no longer constants.

# 目录 Outline

- 背景介绍
  - 嵌套闭合磁面假设
  - 学科分野
  - Poincaré-Hopf 定理
  - Poincaré-Birkhoff 定理
  - 三维磁拓扑相关的实验和模拟研究
  - KAM 定理
  - 现代的共振磁扰动磁谱分析方法
- 流形生长
  - 不变流形的定义
  - 磁力线对初值的敏感性$\mathcal{D}\boldsymbol{X}_{\mathrm{pol}}$
  - $\mathcal{D}\mathcal{P}^{\pm m}$ 在环上的演化和环的分类
  - 生长流形的经典方法和新方法
  - 不变流形的样例演示及解析的例子
- 回顾与展望
  - 边界磁拓扑
  - 最外闭合磁面的确定
  - 拓扑控制

# Physical picture

## 物理图象


When the plasma free energy is below the threshold of the nested tori.
等离子体自由能在嵌套磁面能承受的阈值之内时。

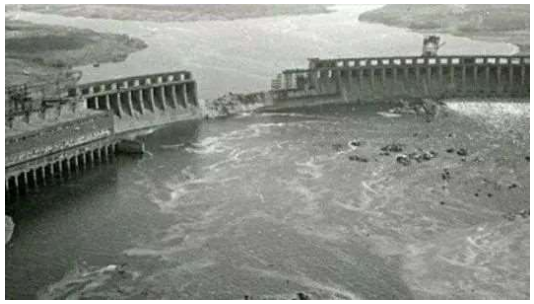

When the plasma free energy is above the threshold of the nested tori.
等离子体自由能超出嵌套磁面能承受的阈值时。

Plasma

Nested tori

- It has a threshold for the free energy it can hold

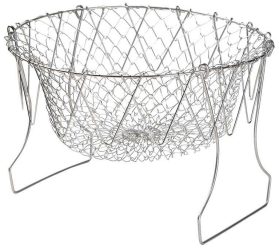

Scrape-off layer
刮削层


First Wall
第一壁

Fig. An analogy picture to magnetically confined plasma

# Edge magnetic topology

## 边界磁拓扑

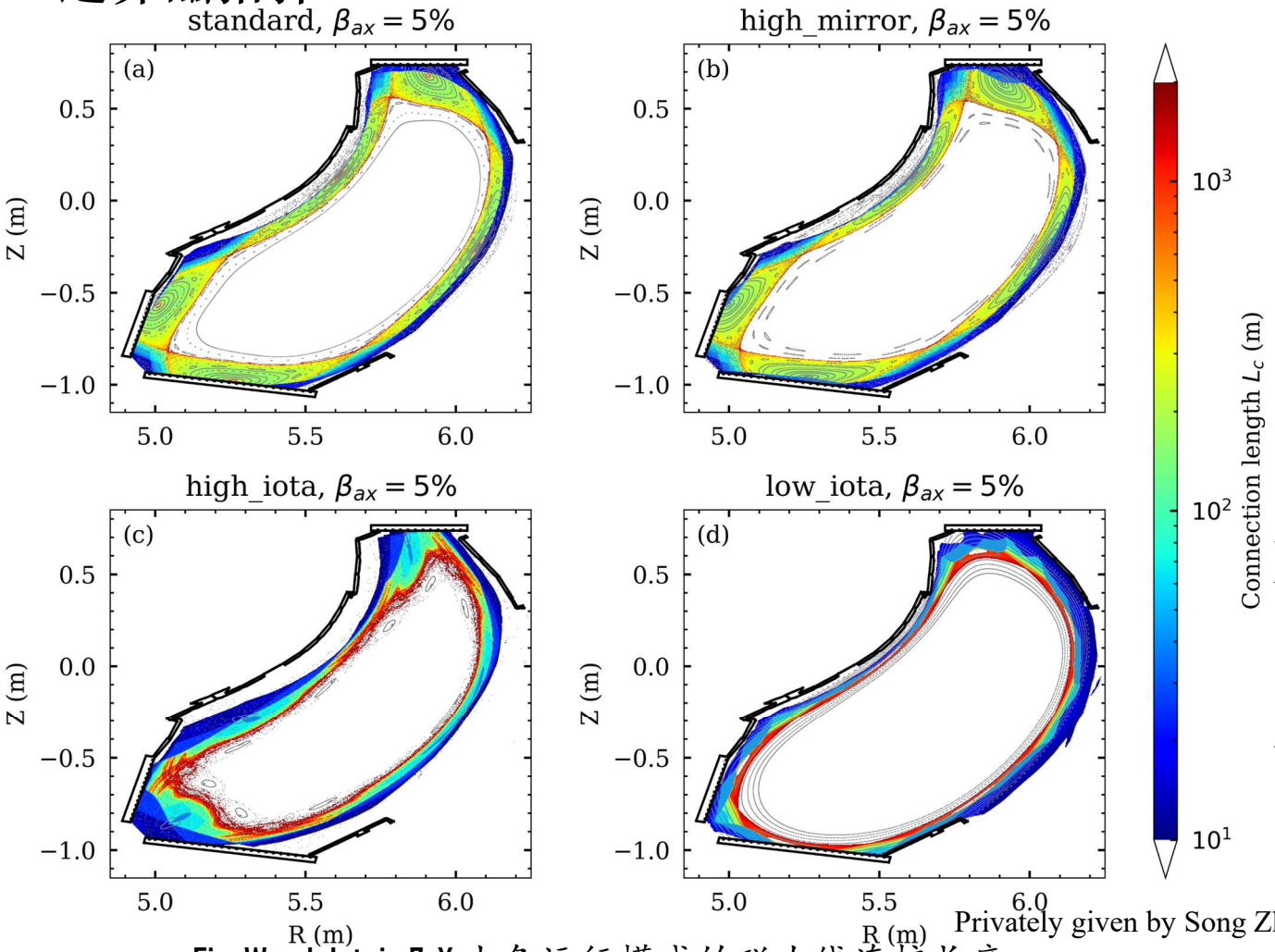


Fig. Wendelstein 7-X 上各运行模式的磁力线连接长度

Privately given by Song Zhou, 2021

T. Eich *et al.* 2013 *Nucl. Fusion* **53** 093031
Scaling of the tokamak near the scrape-off layer H-mode power width and implications for ITER
托卡马克刮削层附近 H 模功率宽度给 ITER 的定标和影响

$\lambda_{q,ITER} \approx 1$ mm

边界复杂的磁拓扑结构对**热流分布**和**边界杂质输运**有重要的研究意义，直接关系到偏滤器的设计。

仿星器中的磁岛偏滤器位型设计直接关系到靶板上**湿区的大小**，高 $\iota$ 位型下的磁力线连接长度分布亦出现复杂的拓扑特征。

# Edge magnetic topology

## 边界磁拓扑

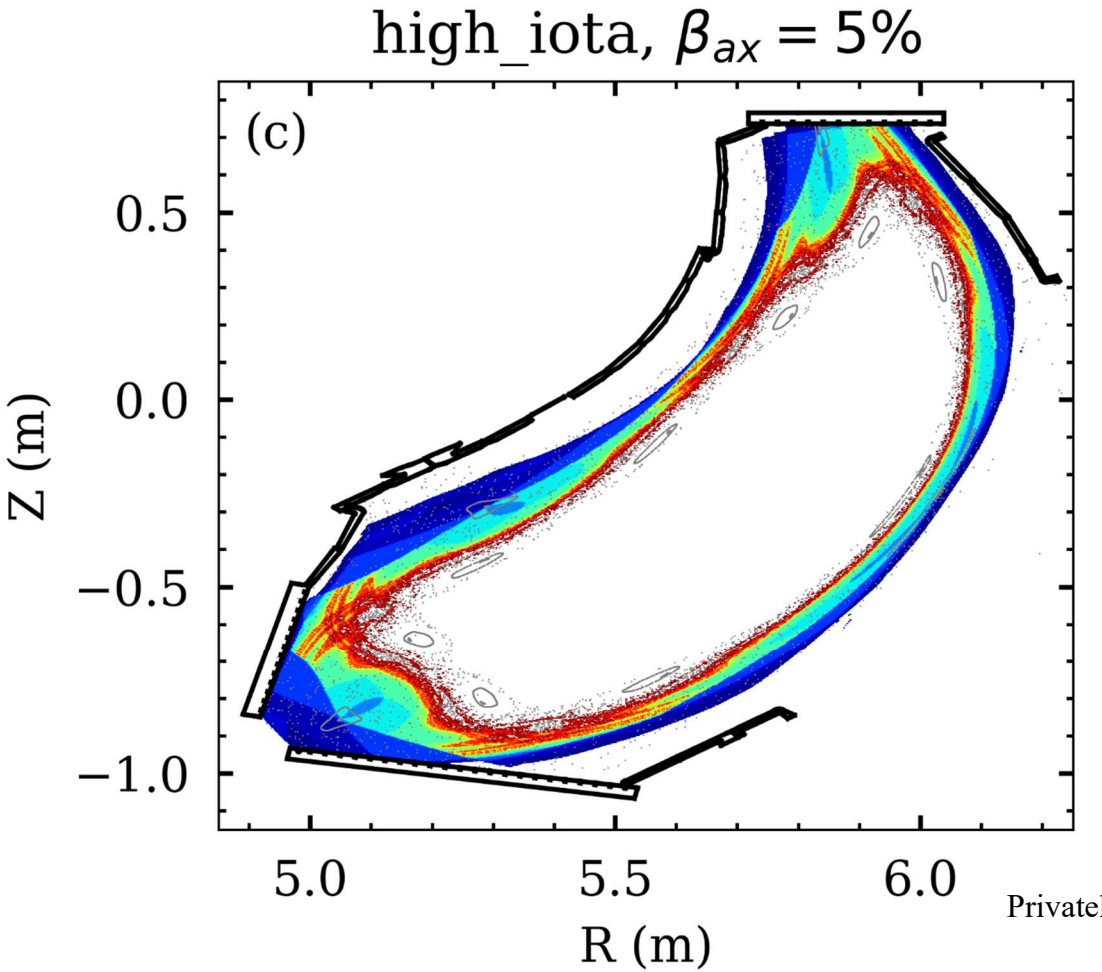


Fig. Wendelstein 7-X 上各运行模式的磁力线连接长度

Privately given by Song Zhou, 2021

边界复杂的磁拓扑结构对**热流分布**和**边界杂质输运**有重要的研究意义，直接关系到偏滤器的设计。

仿星器中的磁岛偏滤器位型设计直接关系到靶板上**湿区的大小**，高 $\iota$ 位型下的磁力线连接长度分布亦出现复杂的拓扑特征。

# How to locate the true LCFS?

## 如何确定真正的最外闭合磁面?

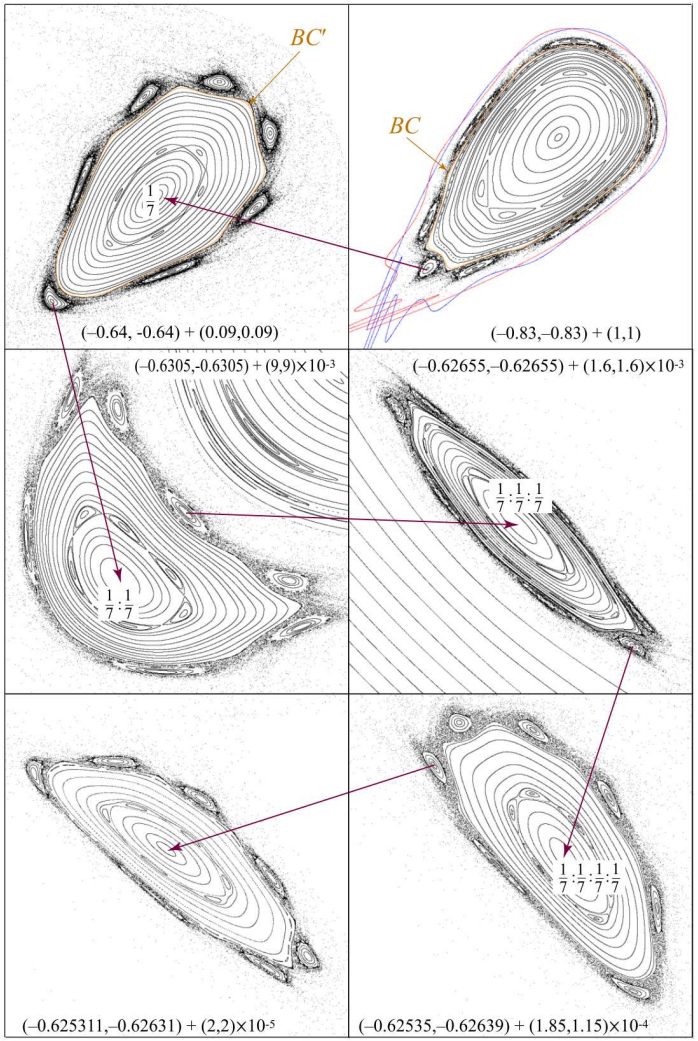


$$R = \frac{1}{4}[2 - \mathrm{Tr}(DT^q)]$$

J. M. Greene, R. S. Mackay and J. Stark, *Physica D*, **21**, 267-295, 1986
Boundary circles for area-preserving maps,
保面积映射的边界圈

$$R = \frac{1}{4}[2 - \lambda_u - \lambda_s]$$

Or Alus *et al* 2014 *Phys. Rev. E* **90** 062923
Statistics of the island-around-island hierarchy in Hamiltonian phase space
Hamilton 相空间中岛外岛层次的统计
Figure from this paper

$$R = \frac{1}{4}[2 - \lambda_u - 1/\lambda_u]$$

- **Greene, Or Alus** 等人称最外的那个环为边界圈（**boundary circle, BC**），他们以二维保面积的映射为研究对象，主要是 **Hénon map**。
- 边界圈对应的旋转数（**rotation number**）是“最无理”的，如果把它拆分成连分数的形式，在某一个 $m_i$ 之后 $m_i$ 全都等于1。

$$\omega = m_0 + \cfrac{1}{m_1 + \cfrac{1}{m_2 + \cdots}} = [m_0; m_1, m_2, \ldots]$$

# From structure to control

## 从结构到控制

EAST 上利用 RMP 实现 ELM 的抑制与偏滤器靶板热流分布动态调节的研

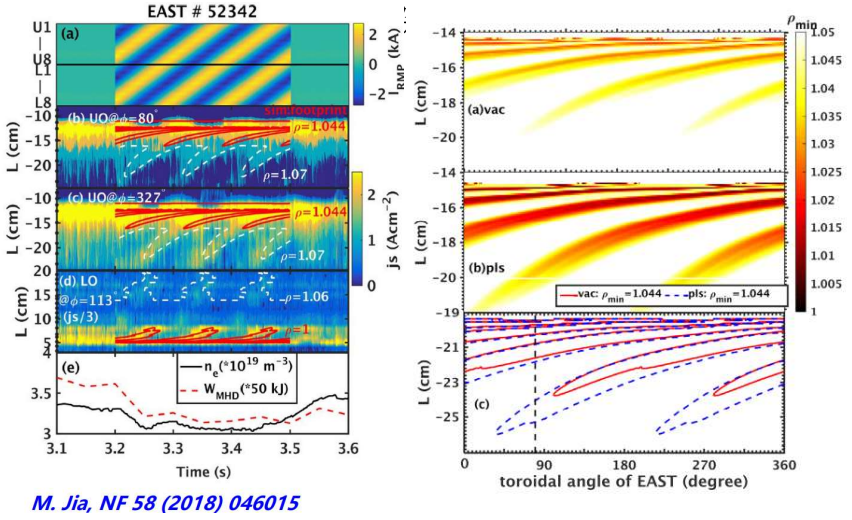


M. Jia, NF 58 (2018) 046015

$$\frac{\partial \boldsymbol{X}^{u/s}}{\partial s} = \frac{\frac{R\boldsymbol{B}_{pol}}{B_\phi} - \frac{\partial \boldsymbol{X}^{u/s}}{\partial \phi}}{\pm \left\| \frac{R\boldsymbol{B}_{pol}}{B_\phi} - \frac{\partial \boldsymbol{X}^{u/s}}{\partial \phi} \right\|_2}$$

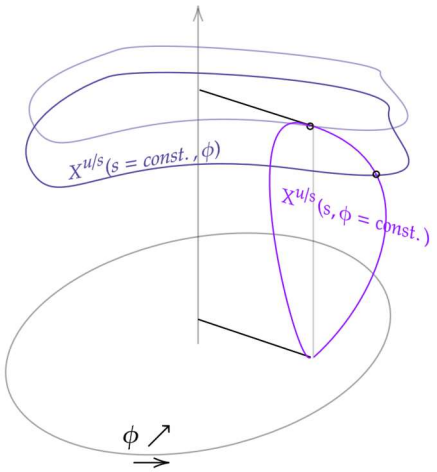


O/X 环控制方程

流形控制公式

看到偏滤器上的带状结构 → 写出流形生长公式 → 主动控制拓扑、调节热负荷

# Topology control

## 拓扑控制

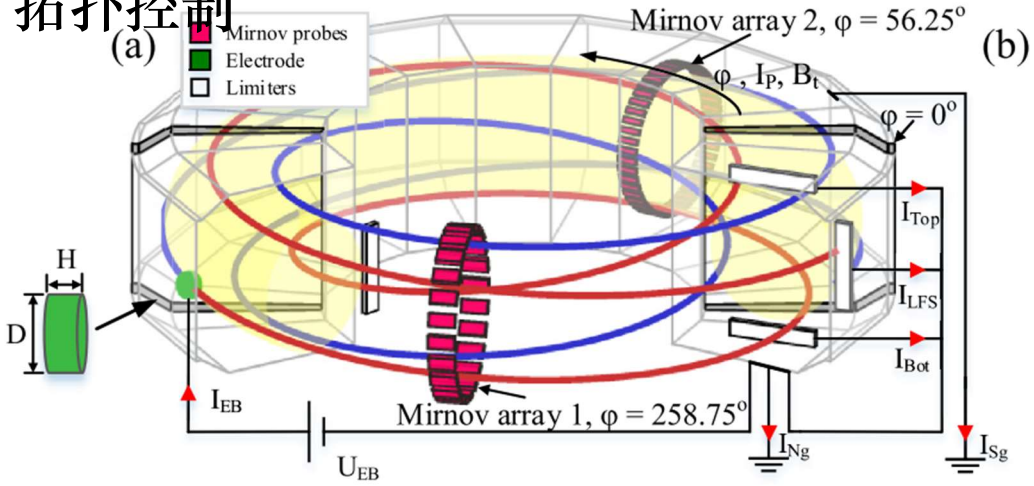


N. Wang et al 2019 *Nucl. Fusion* **59** 096047

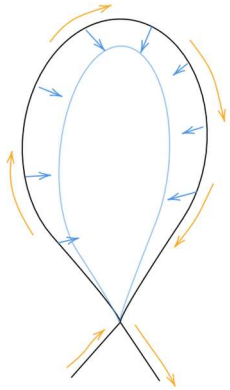

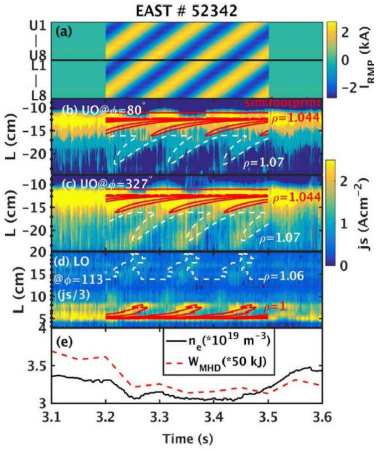


Fig. 流形控制公式控制等离子体的大小的示意图

*M. Jia, NF 58 (2018) 046015*

- 对磁拓扑的自动化控制
  - 偏压电极诱导电流丝，电流丝改变边界磁拓扑，磁力线控制公式控制电流丝
  - 各线圈的集成控制
  - 柱坐标轴对称条件下，X 环控制和流形控制公式更为简单，可用于运行人员控制最外闭合磁面包裹住的等离子体大小
- 调节偏滤器上的热负荷宽度、位置

# Discussion and conclusion

## 讨论和总结

### 不变流形，三维磁拓扑中混沌场的关键结构

- 给**拓扑控制**提供基础
- 帮助研究复杂边界拓扑结构下的输运
- 最外闭合磁面化为两道横截相交流形，我们称为最外鞍环的不变流形 **(invariant manifolds of outmost saddle cycle(s))**
  - 周期性的瞬态爆发 ELM 转为稳定的对流输运
  - Plasma/SOL 分界不再清晰
  - 落入两道流形包围区域的粒子很快会撞到壁上（损失锥大于 $\pi/2$ + 碰撞会导致反向）

### 讨论

- 偏滤器
  - 小心热负荷打到未设计好的地方
  - 热负荷沉积区升至二维，不必局限在一维
- 诊断会关心等离子体边界 $n$ 剖面可能非单调
- 是否可能主动设计磁场，使得边界混沌化且延长磁力线连接长度以改善偏滤器热负荷，同时芯部磁岛尽可能地小。
- 最外闭合磁面退到什么位置？

# 谢谢大家

# Thank you